BSGF - Earth Sciences Bulletin 2024, 195, 2
© A. Atik *et al.*, Published by EDP Sciences 2024
https://doi.org/10.1051/bsgf/2023012

Special Issue Messinian Crisis, ed. Jean-Pierre Suc and Jean-Loup Rubino (Guest Editors)

Available online at:
www.bsgf.fr

Open Access

New insights on the latest Messinian-to-Piacenzian stratigraphic series from the Dahra Massif (Lower Chelif Basin, Algeria): Lago Mare, reflooding and bio-events

Asma Atik[1], Mohamed El Habib Mansouri[1], Mostefa Bessedik[1,*], Mohammed Kamel Osman[1], Lahcene Belkebir[1], Jean-Paul Saint Martin[2], Christian Chaix[2], Ayoub Belkhir[1], Christian Gorini[3], Ahmed Belhadji[1] and Linda Satour[1]

[1] Laboratoire de Paléontologie Stratigraphique et Paléoenvironnement, FSTU, Université d'Oran 2 Mohamed Ben Ahmed, BP 1051, 31 000, Oran El M'Naouer (Algérie)
[2] UMR 7207 CR2P, MNHN-CNRS-SU, Muséum National d'Histoire Naturelle, Département Origines et Evolution, 8 rue Buffon, 75005 Paris, France
[3] Sorbonne Université, CNRS-INSU, Institut des Sciences de la Terre, ISTeP UMR 7193, 75005 Paris, France

Received: 20 April 2023 / Accepted: 22 September 2023 / Publishing online: 8 January 2024

Abstract – Geological investigations carried out on the Dahra Massif have revealed sedimentary changes and bioevents characterizing the post-gypsum detrital sediments (from Messinian to Piacenzian), which are followed by the Trubi equivalent Pliocene marls or white marly limestones.
Structured into two superimposed steps, the late Messinian deposits yielded two successive ostracod assemblages. They indicate a brackish environment for the lower and a fairly open shallow brackish environment for the second. Based on their ostracod content, assemblage 1 (*Cyprideis*, *Loxoconcha muelleri*) corresponds to the Lago Mare biofacies 1 of the Apennine foredeep, which is correlated with the Lago Mare 1 episode dated between 5.64 and 5.60 Ma. Assemblage 2 (*Loxocorniculina djafarovi*) is referred to the Lago Mare biofacies 2 described in the same region. It is correlated with the Lago Mare 3 episode, dated between 5.46 and 5.33 Ma.
Moreover, the stratigraphic succession is marked by a major discontinuity indicated by a hardground, separating step 1 from step 2 and corresponding to the ostracod assemblages 1 and 2, respectively. This discontinuity is considered here to be equivalent to the Messinian Erosional Surface, already evidenced in the region and widely known around the Mediterranean Basin.
These late Messinian deposits and their ostracod assemblage 2, notably the detrital sedimentation with *Ceratolithus acutus*, *Globorotalia margaritae*, *Reticulofenestra cisnerosii* document a marine incursion into the Lower Chelif Basin, corresponding to the latest Messinian marine reflooding of the Mediterranean Basin, that happened before the earliest Zanclean *R. cisnerosii* occurrence. Finally, the bioevents evidenced in the Dahra Massif, reinforce the evidence of the late Messinian Lago Mare 3 episode, and support the ante-Zanclean age of the marine reflooding of the Mediterranean.
The overlying deposits are marked by coral constructions (cf. *Cladocora* cf. *caespitosa*, *Dendrophyllia* sp) never described before and covering the entire early Zanclean, testifying the existence, at that time, of warm enough conditions, which may correspond to the marine isotopic stage TG5.

Keywords: Planktonic microfossils and biostratigraphy / Messinian to Piacenzian / Dahra Massif (Algeria) / Lago Mare / bio-events / coral bioconstructions

Résumé – Nouvelles perspectives sur les séries stratigraphiques du Messinien terminal au Plaisancien du massif du Dahra (Bassin du Bas Chélif, Algérie): Lago Mare, remise en eau et bio-événements. Les études géologiques menées sur le massif du Dahra ont révélé des changements sédimentaires et des événements paléobiologiques caractérisant les sédiments détritiques post-gypse

*Corresponding author: mostefa_bessedik2001@yahoo.fr

(du Messinien au Plaisancien), suivis par des marnes ou des calcaires marneux blancs pliocènes équivalents au faciès Trubi.
Structurés en deux étapes superposées, les dépôts du Messinien terminal ont livré deux assemblages d'ostracodes. Le premier indique un environnement saumâtre et le second un environnement saumâtre peu profond assez ouvert. D'après leur contenu en ostracodes, l'assemblage 1 (*Cyprideis*, *Loxoconcha muelleri*) correspond au Lago Mare biofaciès 1 de l'avant fosse apenninique, qui est corrélé avec l'épisode Lago Mare 1 daté entre 5,64 et 5,60 Ma. L'assemblage 2 (*Loxocorniculina djafarovi*) est rapporté au Lago Mare biofaciès 2 mis en évidence dans la même région. Il est corrélé avec l'épisode Lago Mare 3, daté entre 5,46 et 5,33 Ma.
De plus, la succession sédimentaire est affectée par une discontinuité majeure matérialisée par une surface rubéfiée (*hardground*), séparant l'étape 1 de l'étape 2, correspondant respectivement aux assemblages d'ostracodes 1 et 2. Cette discontinuité est considérée comme l'équivalent de la Surface d'Erosion Messinienne, déjà reconnue dans la région et abondamment décrite tout autour du bassin méditerranéen. Ces dépôts du Messinien terminal et leur assemblage d'ostracodes 2, notamment la sédimentation détritique avec *Ceratolithus acutus*, *Globorotalia margaritae*, *Reticulofenestra cisnerosii* documentent une incursion marine dans le bassin du Bas Chélif, correspondant à la remise en eau marine du bassin méditerranéen au Messinien terminal, avant l'apparition de *Reticulofenestra cisnerosii* indiquant la base du Zancléen.
Ainsi, les bioévénements mis en évidence dans le massif du Dahra permettent-ils de renforcer l'existence du Lago Mare 3 d'âge Messinien terminal et de la remise en eau marine de la Méditerranée antérieurement au début du Pliocène.
Les dépôts sus-jacents sont caractérisés par des constructions coralliennes (cf. *Cladocora* cf. *caespitosa*, *Dendrophyllia* sp) jamais décrites auparavant et couvrant l'ensemble du Zancléen inférieur. Elles témoignent de l'existence, à cette époque, de conditions suffisamment chaudes, pouvant correspondre au stade isotopique TG5.

Most-clés : Microfossiles planctoniques et biostratigraphie / Messinien à Plaisancien / Massif du Dahra (Algérie) / Lago Mare / bio-evenements / bioconstructions coralliennes

1 Introduction

Miocene-Pliocene sedimentation in the Lower Chelif Basin is highly diversified according to its platform to basin facies. The Messinian (7.25–5.33 Ma) is well-known for its pre-reef deposits (Saint Martin, 1990): blue marls, diatomites bearing fish fauna (Arambourg, 1927, Gaudant *et al*., 1997). These deposits evolve vertically into bioclastic sandstones to coralline calcareous algae, leading up to coral bioconstructions (Djebel Murdjadjo: Cornée *et al*., 1994; Saint Martin *et al*., 1995).

The subtropical marine environments characterized by coral reefs (*Porites*, *Tarbellastraea* and *Siderastraea*) as well as impoverished *Avicennia* mangrove (Saint Martin, 1990; Chikhi, 1992) are succeeded by a post-reefal sedimentation including stromatolites, oolitic accumulations and gypsum (Rouchy, 1982a; Saint Martin, 1990; Cornée *et al*., 1994). These sedimentary deposits indicate a degradation of marine conditions and are often associated to the so-called Terminal Carbonate Complex (Esteban, 1979; Cunningham *et al*., 1997; Cunningham and Collins, 2002; Cornée *et al*., 2004; Roveri *et al*., 2009, Roveri *et al* 2020; Clauzon *et al*., 2015).

Pre-evaporitic sediments including diatomites characterize the sedimentary succession seaward of the platform (Rouchy, 1982b). This evolution leads to the formation of gypsum deposits with varying thickness, from a few meters south of the Lower Chelif Basin (Beni Chougrane: Sahaouria) to several hundred meters northward (Tazgaït) and south (Ouled Maallah) of the Dahra Massif. The post-evaporitic facies are diverse (Anderson, 1936; Perrodon, 1957; Welter *et al*., 1959 ; Rouchy, 1982a, b), indicating the onset of a desalination process where environments became palustrine to lacustrine (Rouchy, 1982b; Rouchy and Saint Martin, 1992; Orszag-Sperber *et al*., 2000; Orszag-Sperber, 2006; Rouchy and Caruso, 2006; Rouchy *et al*., 2007).

The Upper Miocene sedimentary succession comprises the Lago Mare biofacies (Anderson, 1936; Perrodon, 1957; Rouchy, 1982b). The chronological context and causative mechanism of such biofacies are still the subject of debate (Gautier *et al*., 1994; DeCelles and Cavazza, 1995; Clauzon *et al*., 1996, 2015; Riding *et al*., 1998; Butler *et al*., 1999; Krijgsman *et al*., 1999; Rouchy and Caruso, 2006; Bassetti *et al*., 2006; Manzi *et al*., 2013; Roveri *et al*., 2014b, 2016; Pellen *et al*., 2017).

The deposition of evaporites occurred in two steps. The first step (5.97–5.60 Ma) involved the deposits of gypsum (sulfates) in the peripheral basins, while the second step (5.60–5.46 Ma) involved the deposit of evaporite giant in the central basins (chlorides: K, Na, and Mg). This second step is believed to correspond to a drop in the Mediterranean Sea level and strong subaerial erosion of its margins (Clauzon *et al*., 1996, 2015; CIESM, 2008; Bache *et al*., 2012; Andreetto *et al*., 2021).

In light of these considerations, Rouchy *et al*. (2007) described several localities corresponding to these facies in the Lower Chelif Basin, including Beni Chougrane (Sig, Sahaouria, El Ghomri) and the Dahra Massif (Djebel Meni-Abreuvoir, Oued El Aicha). Additionally, Osman *et al*. (2021) described similar facies in the Dahra region at Azaizia and Ain Yakoub. These studies instead of authors identified the presence of a Lago Mare (Rouchy *et al*., 2007), also referred to as Lago Mare 1 (Osman *et al*., 2021), during the Messinian Salinity Crisis (MSC). This Lago Mare that has been interpreted as a result of the flow of freshwater coming from

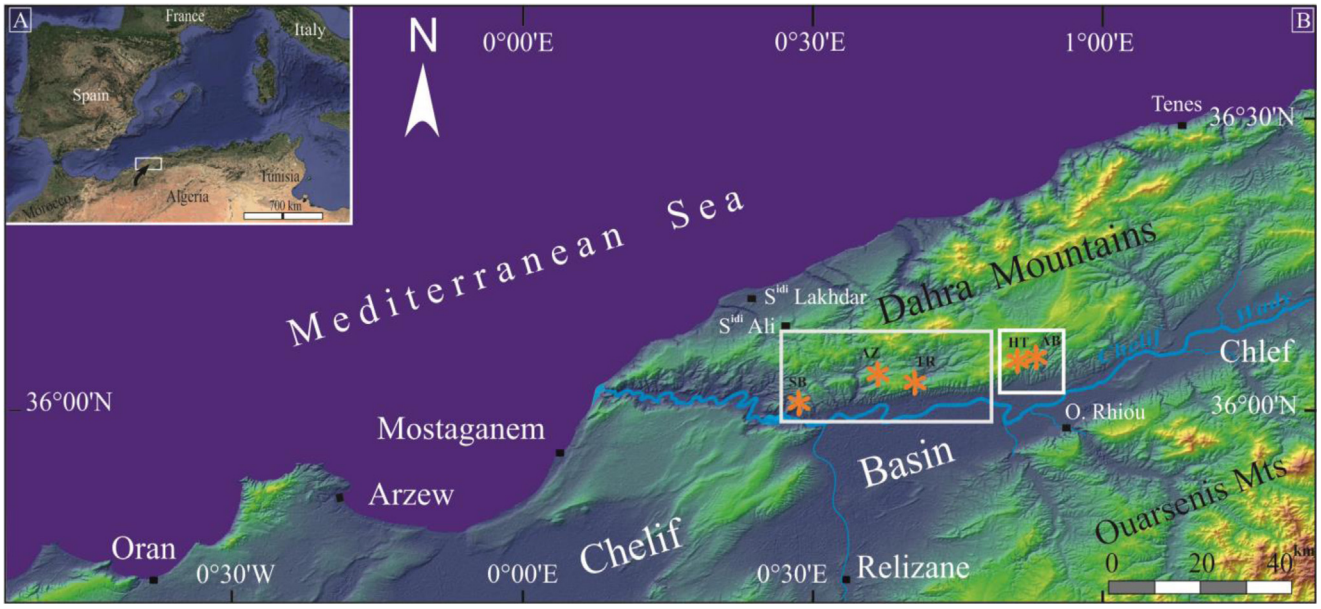

Fig. 1. A: Northwestern Mediterranean region map focusing the studied area; B: Location map of the Miocene-Pliocene series of Ouled Slama and Sidi Brahim Telegraph, southern slope of the Dahra Massif (google map); boxes show the location of geological maps (Fig. 2). Studied and correlated sections with UTM coordinates: SB = Sidi Brahim Telegraph (Zone 31S: 3987031 E, 272327 E); AZ = Azaïzia (Zone 31S: 3990911 N, 285525 E); TR = Tarhia (Zone 31S: 3991563 N, 291432 E); HT = Hgaf Tamda (Zone 31S: 3995721 N, 308899 E); AB = Djebel El Abiod (Zone 31S: 3995798 N, 309644 E).

Fig. 1. A : Carte de la région méditerranéenne nord-occidentale, montrant la zone étudiée ; B : Carte de localisation des séries miocènes-pliocènes des Ouled Slama et du Télégraphe de Sidi Brahim.

the Paratethys into the Mediterranean Sea represents a high sea-level exchange (Clauzon *et al.*, 2005; Snel *et al.*, 2006; Popescu *et al.*, 2009, 2015; Manzi *et al.*, 2009; Suc *et al.*, 2011; Do Couto *et al.*, 2014).

Several times, particularly during two distinct events, Lago Mares (LM1 and LM3) seem to have characterize this water exchange (Clauzon *et al.*, 2005; Popescu *et al.*, 2015). LM1, estimated from 5.64 to 5.60 Ma, overlying peripheral evaporites is affected by the Messinian Erosional Surface (MES) (Gautier *et al.*, 1994; Clauzon *et al.*, 2005; Popescu *et al.*, 2009; Manzi *et al.*, 2009; Clauzon *et al.*, 2015). LM3, following the marine reflooding of the Mediterranean Basin is dated from 5,46 to 5,33 Ma (Krijgsman *et al.*, 2001; Clauzon *et al.*, 2005; Popescu *et al.*, 2007, 2009, 2015; Bache *et al.*, 2012; Do Couto *et al.*, 2014). In addition, a LM2, reported from deep central basins (ca. 5.50–5.46 Ma), is considered as a Paratethys discharge after erosion of the Hellenic Arc or overflow over it (Popescu *et al.*, 2015). Manzi *et al.* (2013) and Roveri *et al.* (2014a, b, 2016) consider that LM1 and LM3 represent in fact a single phase, located between 5.42 and 5.33 Ma, corresponding also to LM2 in the central basins.

The return to normal marine conditions into the Lower Chelif Basin is usually characterized by the widespread occurrence of Zanclean blue marls or "Trubi facies"; whitish in color at the surface. These blue marls are rich in microfauna (Perrodon, 1957; Mazzola, 1971; Belkebir and Anglada, 1985; Thomas, 1985; Belkebir *et al.*, 1996). This transgression appears to have resulted in the inundation of certain morphological structures inherited from the MSC (Dahra: Osman *et al.*, 2021; Oued Rhiou Boukadir: Moulana *et al.*, 2021, 2022). The overlying grey marls are still of Zanclean age and are in turn overlain by Piacenzian alternating marls and sandstones. They are marked by bivalve shell concentrations (Rouchy *et al.*, 2007; Belhadji *et al.*, 2008; Mansouri *et al.*, 2008; Atif *et al.*, 2008; Satour *et al.*, 2013, 2020; Bendella *et al.*, 2021; Satour, 2021; Osman *et al.*, 2021; Benyoucef *et al.*, 2021; Mansouri, 2021).

The present study focuses on the post-gypsum sedimentation (late Messinian – Piacenzian) in the Dahra Massif (Fig. 1), with a particular emphasis on three newly studied sections: Djebel El Abiod, Hgaf Tamda, and Sidi Brahim Telegraph. The results of these sections are supplemented by data from other sections, including the basal part of the Oued Tarhia section. Previous studies have only inventoried deposits with *Globorotalia puncticulata*, more than 200 m above the gypsum (Osman *et al.*, 2021). In this study, the Oued Tarhia section is described in detail with a focus on its lower part (brown to variegated marls, sandy marls and sandstones), overlying the gypsum and capped by the Pliocene marls.

2 Geological context

Structured like an ENE-WSW oriented depression, the intra-mountain (Tellian) basin of the Lower Chelif (Fig. 1) has undergone significant sedimentation during the Neogene and the Quaternary periods. with a thickness that can reach over 4800 m (Brive, 1897; Anderson, 1936; Perrodon, 1957; Mazzola, 1971; Delfaud *et al.*, 1973; Thomas, 1985; Meghraoui *et al.*, 1988; Neurdin-Trescartes, 1992; Arab

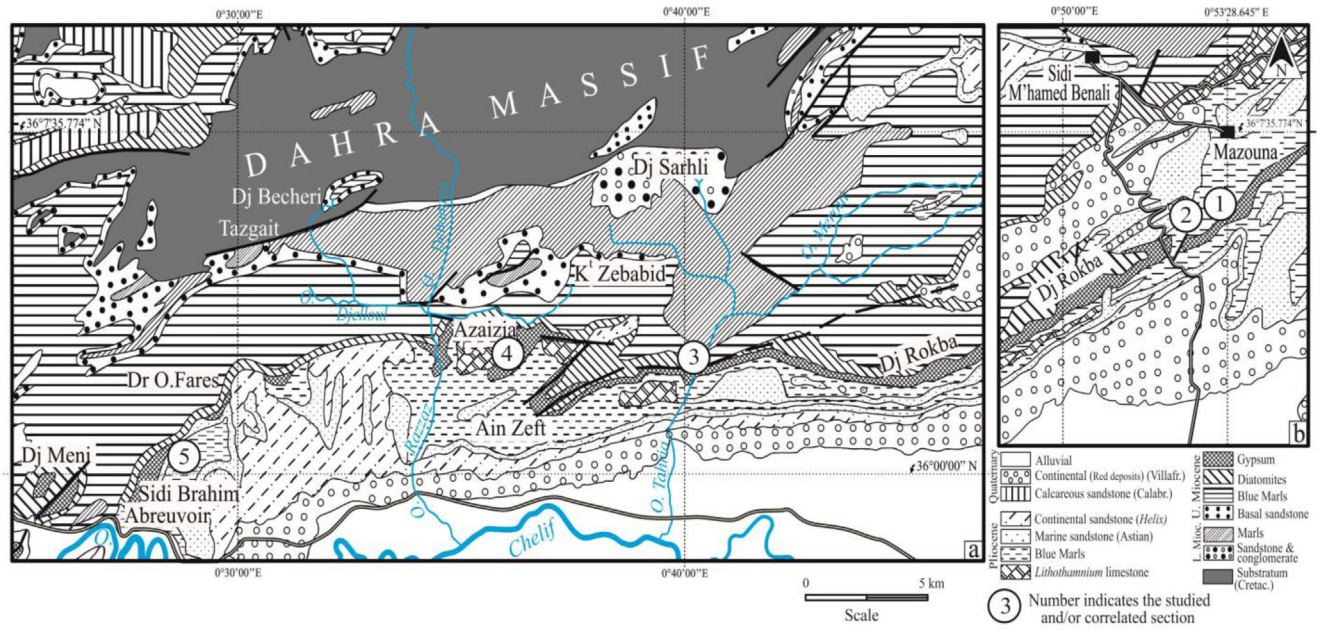

Fig. 2. Geological maps of the Western (a) and Eastern (b) Dahra Massif (partly modified from Perrodon, 1957), showing the Late Miocene to Pliocene lithostratigraphic succession and the location of the studied and/or correlated sections. 1, Djebel El Abiod; 2, Hgaf Tamda; 3, Oued Tarhia; 4, Azaïzia; 5, Sidi Brahim Telegraph.
Fig. 2. Carte géologique du massif du Dahra occidental (a) et oriental (b) d'après Perrodon (1957).

et al., 2015). This region shows evidence of Alpine tectonics, still active today (Guardia, 1975; Meghraoui, 1982; Meghraoui *et al.*, 1986; Meghraoui *et al.*, 1988; Derder *et al.*, 2013; Leprêtre *et al.*, 2018; Abbouda *et al.*, 2018). The structure of the Dahra Massif, in titled blocks, dates back to the end of the Cretaceous (Brive, 1897; Anderson, 1936; Leprêtre *et al.*, 2018). In relation to this, numerous authors have contributed to the understanding of the Cenozoic stratigraphy of this basin and the surrounding Tell massifs (Pomel, 1892; Brive, 1897; Anderson, 1936; Perrodon, 1957).

With regard to the Miocene marine sedimentation of this region, two major sequences are distinguished (Delfaud *et al.*, 1973; Thomas, 1985; Neurdin Trescartes, 1992); they generally correspond to the first and second post-nappe cycles (Perrodon, 1957; Meghraoui, 1982; Meghraoui *et al.*, 1988; Fig. 2). Their ages are estimated from late Burdigalian to Serravallian (Belkebir and Anglada, 1985; Belkebir *et al.*, 1996; Bessedik *et al.*, 2002; Belkebir *et al.*, 2008) concerning the first sequence and from Tortonian to Messinian concerning the second one (Mazzola, 1971; Neurdin-Trescartes, 1992, 1995; Belkebir *et al.*, 2008; Belhadji *et al.*, 2008). Continental sedimentation is also widespread on the southern and northern margins of the Lower Chelif Basin, in addition to the marine sedimentation areas (Guardia, 1975, 1976; Ouda and Ameur, 1978; Ameur-Chehbeur, 1992; Bessedik *et al.*, 1997; Bessedik *et al.*, 2002; Belkebir *et al.*, 1996; Mahboubi *et al.*, 2015).

The Late Miocene sedimentation is characterized by an unconformity covering earlier marine and continental deposits; it shows a transgressive to a regressive trend (Fig. 2). It consists of marls evolving to diatomite and diatomitic marl alternation, then evaporites and finally post-evaporitic lagunal sediments (Anderson, 1936; Perrodon, 1957; Rouchy, 1982a, b; Thomas, 1985; Saint Martin, 1990; Neurdin-Trescartes, 1992, 1995; Mansour *et al.*, 1999, Rouchy *et al.*, 2007).

The gypsum, which marks the start of the MSC in the Mediterranean peripheral basins, can reach thicknesses of up to 4 meters in some places (with 2 beds) or even more than 250 to 300 meters in the Lower Chelif Basin (massive gypsum), particularly on the southern and northern slopes of the Dahra Massif (Ouled Maallah, Tazgaït: Fig. 2). In the central part of the Basin, post-evaporitic Messinian sedimentation evolved into palustrine to lacustrine deposits. The Pliocene is characterized by "Trubi facies" and marine blue to whitish marls, well represented in the Sidi Brahim Telegraph section with thicknesses up to 750–800 m (Brive, 1897; Anderson, 1936; Perrodon, 1957; Mazzola, 1971; Fenet and Irr, 1973; Belkebir and Anglada, 1985; Thomas, 1985; Neurdin-Trescartes, 1992; Rouchy, 1982a; Rouchy *et al.*, 2007; Atif *et al.*, 2008; Abbouda *et al.*, 2018). In fact, many authors describe compressive tectonics that affected the Pliocene cycle, with some faults still being active (Perrodon, 1957; Thomas, 1985; Meghraoui, 1982; Meghraoui *et al.*, 1988; Derder *et al.*, 2013; Arab *et al.*, 2015; Abbouda *et al.*, 2018).

3 Material and methods

The dating of the Messinian and Pliocene deposits specified, particularly with regard to the northern and southern margins of this basin. Since several works have highlight the diversity of facies and identified several Messinian and Pliocene bioevents in the planktonic foraminifera and calcareous nannoplankton (Saint Martin, 1990; Rouchy *et al.*, 2007; Atif *et al.*, 2008; Osman *et al.*, 2021). These bioevents are calibrated on radiometric and/or astronomic ages

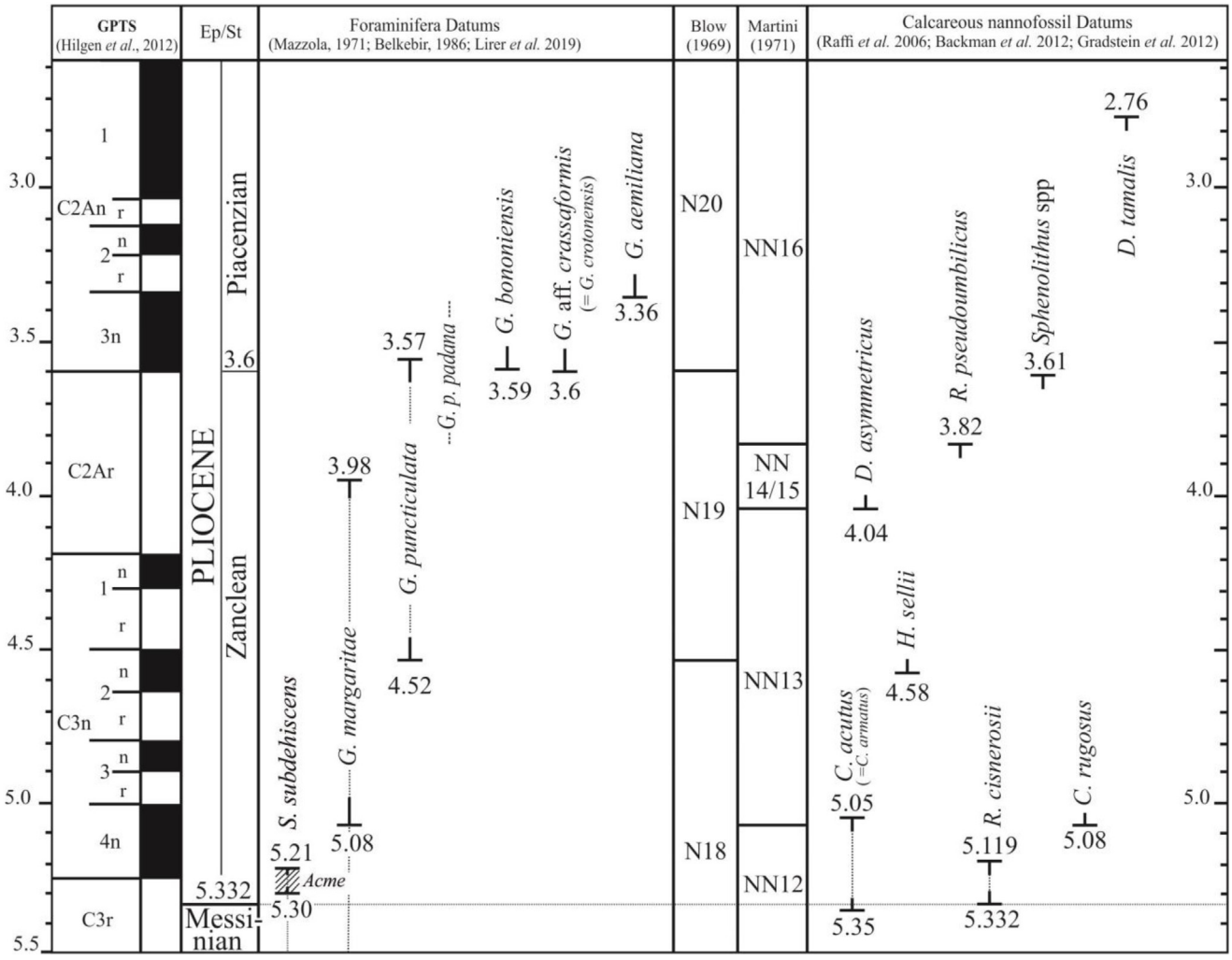

Fig. 3. Chronologically calibrated bioevents identified in the geological series of Ouled Slama and Sidi Brahim Telegraph (Dahra Massif, Lower Chelif Basin). *G. puncticulata padana* Dondi & Papetti 1968: https://www.mikrotax.org/pforams/index.php?id=131261.
Fig. 3. Bio-événements dans la série des Ouled Slama et du Télégraphe de Sidi Brahim.

(Channell *et al.*, 1988, 1992; Sprovieri, 1993; Lourens *et al.*, 2004, 2005; Sprovieri *et al.*, 2006; Raffi *et al.*, 2006; Di Stefano and Sturiale, 2010; Backman *et al.*, 2012; Gradstein *et al.*, 2012; Lirer *et al.*, 2019) (Fig. 3).

This study addresses the post-gypsum deposits located near Hassi Ben Mekki quarry (central Dahra) (RN90) (Djebel El Abiod and Hgaf Tamda sections). Other sections are partially detailed (bottom of the Oued Tarhia section) for their biostratigraphic interest (Messinian-Pliocene boundary). The Sidi Brahim Telegraph section is explored upwards (Pliocene) and enable correlations with the Azaïzia section (a). The boundaries between lithostratigraphic (sub)units have been sought and carefully described.

The extraction of planktonic foraminifera and calcareous nannofossils was performed on the same samples. Due to their significant thickness, more than 50% of the sampling concerned the Djebel El Abiod and Sidi Brahim Telegraph sections. A large number of samples were taken (over 250), but only 190 were selected for their microfossil content. The extraction of foraminifera involves a phase of deflocculation of 200 to 300 grams of sediment, achieved by soaking in lukewarm water. Washing is carried out under a trickle of water through a sieve with a mesh size of 80 and 100 μm. Foraminifera, ostracods, charophytes are identified using a binocular microscope, with magnification ranging from x250 to 500. Extraction of calcareous nannofossils (smear slides) consists in placing a fragment of sediment on a slide before dilution with a drop of distilled water. The slide is stored on hot plate for drying for a few seconds and finally covered with a coverslip, glued using Eukitt resin. The slide is analyzed using a polarizing optical microscope (magnification ×500). The analysis is done by systematically scanning the slide. After targeting the organisms, the determination was carried out with a magnification of ×500 to ×1000 μm.

Our objective is to first specify a reliable stratigraphic framework based on all available data on foraminifera and calcareous nannoplankton in the Miocene and Pliocene marine deposits from the Lower Chelif Basin (Magné in: Perrodon, 1957; Bizon in: Thomas, 1985; Belkebir and Anglada, 1985; Rouchy, 1982a, b; Saint Martin, 1990; Bizon in: Neurdin-Trescartes, 1992; Osman *et al.*, 2021). The planktonic foraminifera bioevents recorded in the Lower Chelif Basin

constitute an important background for the reconstruction of the local biostratigraphy, which is correlated with those established in the Mediterranean (Bizon and Bizon, 1972; Zachariasse, 1975; Cita, 1975; Thunell, 1979; Langereis and Hilgen, 1991; Hilgen *et al*., 2012; Iaccarino *et al.*, 2007) as reported on the standard Blow scale (Blow, 1969). Our biostratigraphy is also based on calcareous nannofossils correlates with the scale proposed by Martini (1971) and Backman *et al*., (2012). Some microfossils constitute, for the base of the Pliocene, important landmarks in relation to the top of the *Sphaeroidinellopsis subdehiscens* acme, reported at 5.21 Ma and 5.30 for its base (Lourens *et al*., 2005; Lirer *et al.,* 2019). *Globorotalia. margaritae* and *Ceratolithus acutus* can also date together the latest Messinian layers.

4 Results

Four geological sections carried out on the southern edge of the Dahra Massif are described in distinct lithostratigraphic units, showing their detailed sedimentological and paleontological contents.

Chronologically, they cover the Upper Miocene and the Pliocene periods. The Djebel El Abiod section is composed of six units (Fig. 4; S1), which respectively belong to Messinian (Units I-III and IV), early Zanclean (Unit V; coral facies), late Zanclean (*p.p.*) and early Piacenzian (Unit VI). The Hgaf Tamda section (Fig. 5; S2) crops out in a syncline with NE-SW oriented axis with five lithostratigraphic units: units I-III are attributed to Messinian, units IV (coral facies) and V belong to Pliocene. The Oued Tarhia section (Fig. 6; S3) is composed of five lithological units: units I-IV and V *p.p.* belong to Messinian; upper part of unit V is integrated within Zanclean. The Sidi Brahim Telegraph section (Fig. 7; S4) is subdivided into four units dated from latest Messinian (UI-II) to Zanclean (UIII) and Piacenzian (Unit IV).

4.1 Post-gypsum deposits or Lago Mare

The post-gypsum sediments, well represented in the Djebel El Abiod section (S1), are reduced or even absent in the Hgaf Tamda (S2) and Oued Tarhia (S3) sections. Their extension reveals, from East to West, a discontinuity in their facies and an irregularity of their topographic background. Two steps characterize this sedimentary succession, which unconformably overlies the selenite gypsum (Fig. 8).

4.1.1 Step 1

It is represented by variegated clays corresponding to a filling sedimentary sequence (clay-sandy marls-sandstone-conglomerates), witness to intense erosion (Fig. 4). Ostracofauna is abundant (Pl. 1): *Cyprideis* (**assemblage 1**) associated with *Loxoconcha muelleri, L.* sp.1 and *L.* sp.2 indicates a brackish, shallow environment attesting some episodic fluvio-lacustrine contributions (*Chara* cf. *hispida*, *Pseudocatillus* sp., and quartz). This ostracofauna (S1) is of late Messinian age (Gliozzi, *pers. comm.*), comparable to that described by Rouchy *et al*. (2007) in the Beni Chougrane (Djebel Touakas), and in the Dahra Massif (Oued El Aïcha).

4.1.2 Step 2

Grey ruby clays are marked by a late Messinian ostracod **assemblage 2** (Gliozzi, *pers. comm.*) over green marine marls with dwarf planktonic foraminifera (Djebel El Abiod): *Loxocorniculina djafarovi*, *Euxinocythere praebaquana*, *Amnicythere* cf. *accicularia*, *A.* sp., *Cytherura pyrama*, *Camptocypria* sp., *Zalanyiella venusta* (Pl. 1). Above, variegated clays have yielded another assemblage with *Cyprideis* (abundant), *Tyrrhenocythere* cf. *ruggierii*, *Amnicythere* sp., *Zalanyiella venusta* (see S1). This **assemblage 2** corresponds to open shallow to brackish marine conditions (*L. djafarovi*), which became brackish to slightly lacustrine (hypo-mesohaline, 5-15‰) at the top (*Cyprideis* abundant). This deposit is unconformably overlain by marine sandy marls (SM1, SM2) containing planktonic foraminifera.

The ostracod association of Djebel El Abiod (Fig. 4) is slightly different from that revealed in the Oued Tarhia (Fig. 6). The T16 sample assemblage (*Loxocorniculina djafarovi*, *Euxinocythere praebaquana*, *Amnicythere* sp., *Cytherura pyrama*, *Loxoconcha muelleri*, *Tyrrhenocythere* cf. *ruggierii*), is different from that from the T17 sample (*Cyprideis*, *Loxoconcha* sp.1, *L.* sp.2, *Tyrrhenocythere pontica*, *Amnicythere* sp., *Amnicythere propinqua,* showing a red gangue on some reworked individuals of *Loxoconcha muelleri*). In addition, the *L. djafarovi* assemblage (Djebel El Abiod) evolves at the top into assemblage with *Cyprideis* (abundant), comparable to that, in the same position, of the Oued Tarhia section (*Cyprideis*, *Loxoconcha* sp .1, *L.* sp.2, *Tyrrhenocythere pontica*, *Amnicythere propinqua, A.* sp.).

The *Loxocorniculina djafarovi* assemblage described in the Sidi Belattar and Sidi Brahim Telegraph sections by Atif *et al.* (2008) seems to present some reworking (*Loxoconcha muelleri*). Not far from this locality, the ostracod assemblages, collected in the Oued Tarhia section (Fig. 6, S3), give rise to similar remarks, in particular the presence of several individuals (shells *in situ*) belonging to *Loxoconcha muelleri* (sample T16), having provided the *L. djafarovi* association. The sample T17 shows individuals of *L. muelleri* with carapaces within a red gangue that suggests their reworking. These observations firstly concern the presence of *L. muelleri* (*in situ*) within the *L. djafarovi* assemblage, mainly in the western localities (Sidi Belattar, Sidi Brahim Telegraph: Atif *et al*., 2008; Oued Tarhia: this work). Secondly, the assemblage with *L. djafarovi* occurs without *L. muelleri* in the sections of Djebel Meni −Abreuvoir (Rouchy *et al*., 2007) and Djebel El Abiod.

The assemblage of *Cyprideis* associated with *L. muelleri* (**assemblage 1**) followed by that of *L. djafarovi* (**assemblage 2**) constitutes a chronological landmark succession in the Lower Chelif Basin and the Dahra Massif.

The grey ruby and variegated clays of Djebel El Abiod (step 2), marked by a brackish character, are interrupted by an unconformity and overlain by marine sandy marls (SM1, SM2). These latter have yielded foraminifera and calcareous nannofossils from Miocene to Pliocene with a strong planktonic representation (*Globigerinoides*, *Globigerina*, *Globorotalia*, *Coccolithus pelagicus*, *Helicosphaera carteri*, *Discoaster variabilis* and some *Sphenolithus*), before the emplacement of Pliocene deposits. This marine episode seems to correspond to the grey sandy marls with *Globorotalia* gp,

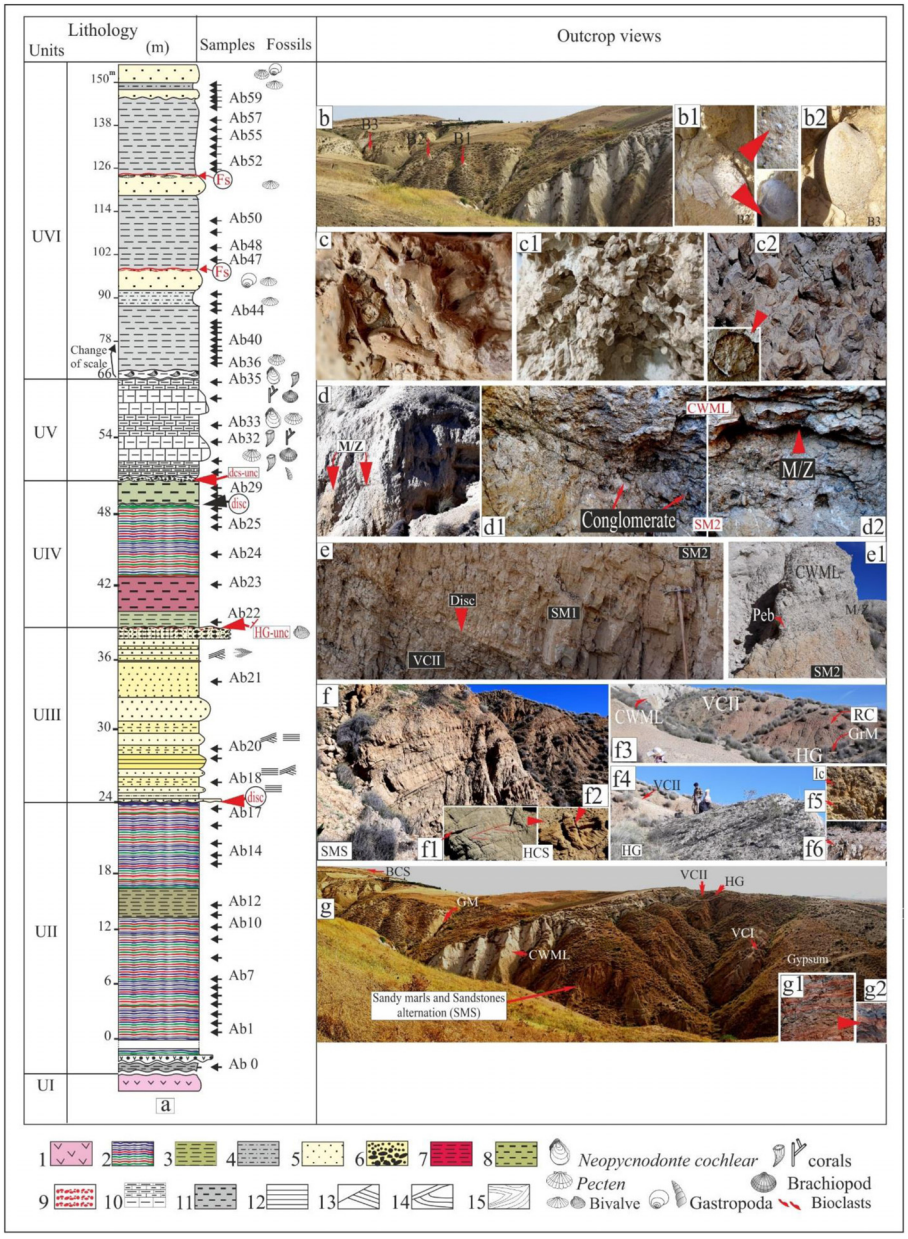

Fig. 4. Geological section of Djebel El Abiod (Dahra). – Illustrated lithology and paleontological contents from the base to the top: Gypsum (1); Variegated (varved) clay (2); Green clay (3); Sandy clay (4); Sandstone (5); Conglomerate (6) ; Ruby clay (7); Green marl (8) ; Microconglomerate (9) ; Coralliferous white marly limestone (10) ; Gray marls (11) ; Plane stratification (12); Oblic stratification (13) ; Cross bedding (14); Hummocky cross stratification (15) ; Dis = discontinuity; HG = Hardground; Dcs = Double corrugated surface; Fs = Ferruginous surface. a: Djebel El Abiod geological section. b: Panoramic view of the upper section of the grey marls with three sandy marl fossiliferous bars (B1, B2, B3). b1: Broken shell test (B2), top right (B3): Mollusk test (Amussium?), at the bottom right (B3): broken shells (Pectenidae, Amussium? among others). b2: internal cast of Veneridae (B3). c, c1: Scleratinian coral (cf. Cladocora cf. caespitosa). c2: *Dendrophyllia*. sp. and details. d: bottom view of the coralliferous white marly limestone (CWML = Unit V) showing M/Z = Messinian-Zanclean boundary. d1, d2: Detail of intermediate conglomerate between the CWML Unit V and SM2 Unit IVd (see S1) corresponding to a double corrugated surface (dcs); base of Zanclean CWML indicated by M/Z. e: Boundary between variegated clays (VCII) and sandy marls (SM1); sedimentary discontinuity (facies change); with a slight angle angular. e1: The upper sandy marls (SM2) and the CWML bottom indicating the Messinian-Zanclean boundary (M/Z); intermediate conglomerate, pebbles and yellow sandy marls. f: Sandy marls and sandstone (Unit III) showing (details) hummocky cross stratification. f1, f2: Hummocky cross stratification (HCS). f3: Panorama showing post-hardground (HG) sedimentation: green marls (GrM), ruby clay (RC), variegated clays II (VCII) and Corlliferous white marly limestone (CWML). f4: waped structure of the Hardground, VCII. f5, f6: HG surface showing conglomerates with calcareous matrix (f6) or partially eroded iron crust. g: Panoramic view of the lower section showing the disposition of stratigraphic units (gypsum, VCI; Variegated clays I, SMS alternation: Sandy marls and Sanstones, HG: Hardground, VCII: Variegated clys II, CWML: Coralliferous white marly sandstone, GM: Grey marls, and BCS: Biodetrital calcareous sandstone). g1: variegated clays I, and details, (VCI).

Fig. 4. Coupe de Djebel El Abiod.

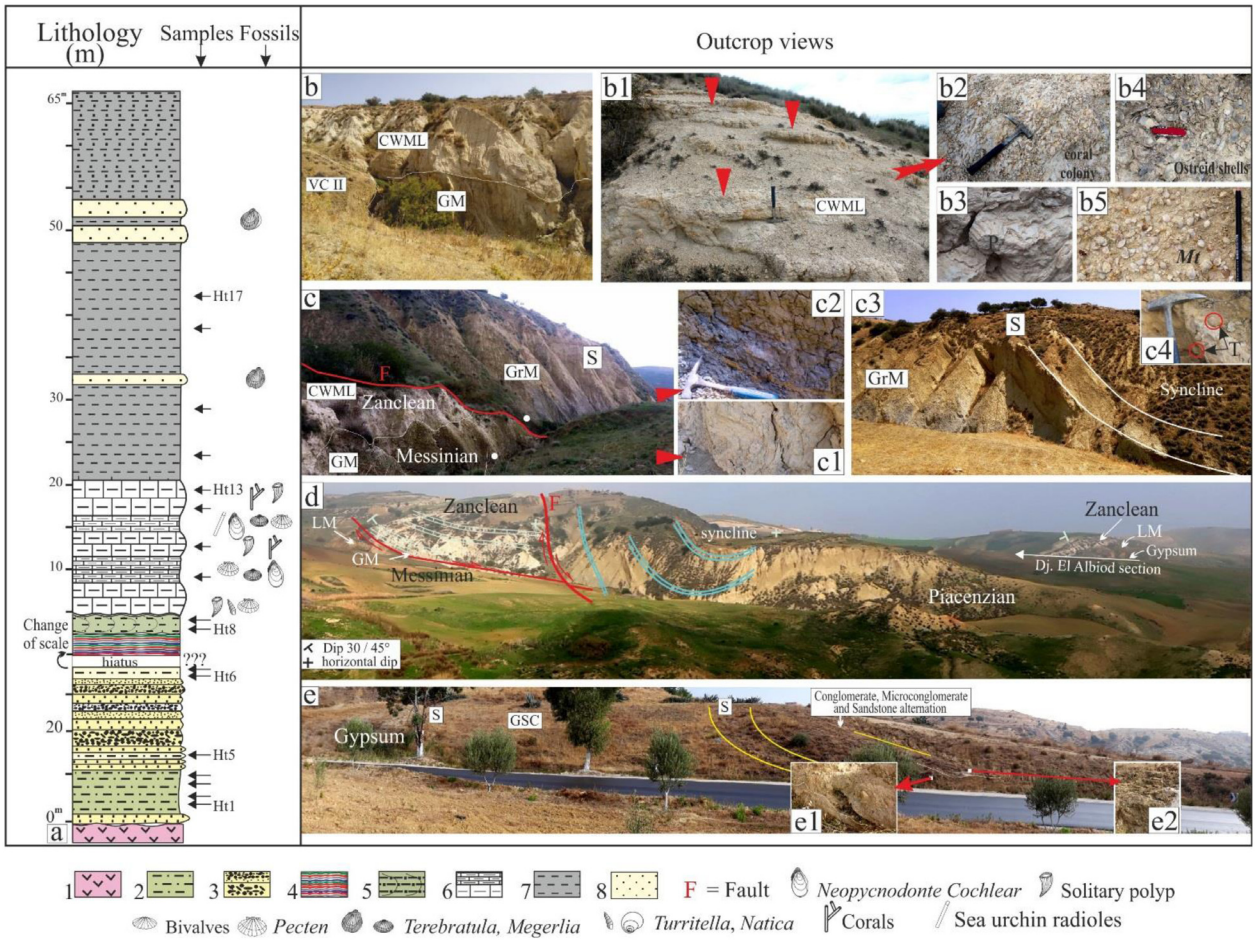

Fig. 5. Geological section of Hgaf Tamda (Dahra). – Lithostratigraphic succession. 1: Gypsum; 2: Green sandy marls; 3: Conglomerates, 4: Variegated clays (varves); 5: Green (sandy) marls; 6: Coralliferous white marly limestone; 7: Grey marl; 8: Sandstone; S = Sandstone; GSC = Green sandy clay; GM = Green marls; LM = Lago Mare; CWML = Coralliferous white marly limestone; GrM = Grey marls; VCII = Variegated Clay II. a: Log showing lithostratigraphic succession. b: Bundary between coralliferous white marly limestone and green marls, position of the variegated clay II (VCII). b1: Panoramic view of coralliferous white marly limestone. b2: Coral facies (coral colony). b3: Facies of solitary corals in marly limestone. b4: Ostreid shell concentrations. b5: *Megerlia truncata* (*Mt*) concentration. c: View showing in the lower left : Messinian-Zanclean boundary (green marls – coralliferous white marly limestone: GM/CWML); in upper right: grey marls (GrM) and sandstone fossiliferous bars (S) of Zanclean age. c1: Knee fold in the green marls (GM). c2: Blue and yellow horizons at the uppermost Zanclean (grey marls). c3: Grey marls (GrM) evolving into fossiliferous sandstone bars (S) constituting a syncline structure. c4: Details in the sandstone bar macrofauna (red circles: *Terebratula* sp.). d: Panoramic view the Hgaf Tamda syncline in the foreground, red lines and arrows indicate fault structures and movement direction of the compartments ; the background shows the transect of the Djebel El Abiod section. e: Panoramic view of the lower part (bottom) of the Hgaf Tamda section on the RN90: gypsum crowned by detrital sedimentation (sandstone, green sandy clays, sandy marls evolving to conglomerates, microconglomerates and sandstones alternation). e1: Detail: transition from sandstone to heterogeneous conglomerates. e2: Detail: transition of conglomerates to channeled sandstone.
Fig. 5. Coupe du Hgaf Tamda.

G. margaritae, *Globigerinoides* gp, *Globigerina* gp, and *Reticulofenestra pseudoumbilicus*, belonging to the Sidi Brahim Telegraph section (Pl. 1).

The lithologic and paleontological successions (step 1, step 2), characterized by brackish or brackish to slightly lacustrine environments are correlated with the gypsum and post-gypsum sedimentation attributed to Lago Mare (Rouchy *et al.*, 2007) even partly to the Lago Mare 1 (Osman *et al.*, 2021) from late Messinian.

Three pre-Zanclean discontinuities are recorded (latest Messinian) in the neighbouring localities of Djebel El Abiod and Hgaf Tamda (Figs. 4 and 5). They locate between: (i) the lower variegated clays and the alternating sandy marl and sandstone (VCI/SMS), (ii) the top of the hardground with distorted structure, belonging to the sandy marls and sandstones and the green marine marls and, (iii) the variegated clays and the marine sandy marls (VCII/SM1).

The most important discontinuity (ii) is recorded in the Djebel El Abiod section (Fig. 4). It is materialized by the surface of the hardground with its subsequent deformation that resulted in varying dip from 25 to 30° towards the NNW, prior to the overlying deposits; we consider it as a major discontinuity equivalent to the Messinian Erosional Surface (MES). It is also underlined by a paleontological change, separating the

pre-hardground **assemblage 1** from the post-hardground **assemblage 2**; this is clearly visible in the Hgaf Tamda, Oued Tarhia and Sidi Brahim Telegraph sections (Fig. 8).

4.1.3 SM1, SM2, Conglomerate and age of Djebel El Abiod

Two sandy marl levels belonging to the Unit IV (SM1, SM2: Fig. 4; S1) rest unconformably on the post-hardground variegated clays (Fig. 4: e: VCII/SM1; e1: SM2, M/Z boundary), which are estimated as latest Messinian in age based on its own ostracod assemblage 2 (Gliozzi, *pers. com.*). Their microfossils show an extensive representation of planktonic foraminifera and calcareous nannofossils (*Globigerinoides*, *Globigerina*, *Globorotalia*, *Coccolithus pelagicus*, *Helicosphaera carteri*, *Discoaster variabilis* and some *Sphenolithus*), witnesses of a marine incursion whose age may be Messinian to Zanclean based on the calcareous nannoflora. These deposits (SM1, SM2) are crowned by an undulating surface (unconformity) overlain by a thin conglomeratic level (Fig. 4: d1, d2 and e1: intermediate conglomerate), the top of which is also interrupted by another undulating surface (called dcs = double corrugated surface, see Fig. 4: a). The overlying deposit is a coralliferous white marly limestone (CWML), which yielded *Globorotalia margaritae*, *Reticulofenestra cisnerosii* of earliest Zanclean age. The latter are correlated with the lower part of the white marls of the Sidi Brahim Telegraph section whose extreme base reveals the presence of *Ceratolithus acutus* (TSB9), followed (Fig. 7, S4) by the presence of *Reticulofenestra cisnerosii* (TSB11).

The age of the conglomerate could be estimated between the late Messinian and the earliest Zanclean. It must locally express the gap of the *Sphaeroidinellopsis subdehiscens* biozone, commonly recognized in the Lower Chelif Basin (Mazzola, 1971; Belhadji *et al*., 2008), possibly incomplete in some places (Rouchy *et al*., 2007; Osman *et al*., 2021). This attribution can be supported by the succession of *C. acutus* (samples T18, T19, T20) and *Globorotalia margaritae* (T19, T20), observed in the Oued Tarhia (S3; Fig. 6). These deposits evidence that the marine reflooding happened prior to the *R. cisnerosii* occurrence (T20). Thus, the data outlined above corroborate dating of the ostracod assemblage 2 highlighted in the Dahra Massif sections and confirm, by correlation, its ascription to the late Messinian.

Consequently, the unconformity and the conglomeratic level observed in the Djebel El Abiod and Hgaf Tamda sections separating the coralliferous white marly limestones from the underlying marine sandy marls (*i.e.,* SM1 and SM2) could be Miocene to Pliocene in age. In the absence of biomarker, the marine sandy marls (SM1 and SM2) are attributed to the late Messinian, which must correspond again or partly to the marine reflooding in the Lower Chelif Basin, coeval with the Lago-Mare assemblage 2 with *Loxocorniculina djafarovi* (latest Messinian) described in the Djebel El Abiod section.

4.2 Coral bioconstructions, associated fauna, age and environment of white marly limestones

The restoration of marine conditions in the Dahra Massif began in the latest Messinian with significant sedimentation of grey sandy marls, generally detrital at the base and recorded in quite deep areas. Other shallow areas are marked by the development of carbonate platforms materialized by lenticular white limestone with *Neopycnodonte cochlear* or algae (*Lithothamnium*) (Brive, 1897; Perrodon, 1957). These deposits include also scaphopods, echinoderms, ostreids, etc.

The extensive exploration of Miocene and Pliocene outcrops in the Dahra Massif allows obtaining new paleontological and stratigraphic data for these white limestones, particularly in the Djebel El Abiod and Hgaf Tamda sections (Figs. 4 and 5). These sediments, unconformable on the Messinian deposits, present alternations of coralliferous white limestone beds and marly limestone (CWML) with abundant specimens of *Neopycnodonte cochlear, Megerlia truncata* and some lenticular clusters of scleractinians evolving to coral bioconstructions with *Dendrophyllia* sp. and cf. *Cladocora* cf. *caespitosa*. These CWML and coral bioconstructions are dated from the early Zanclean, according to the record of *Globorotalia margaritae* (biozone N18 *p.p.*: Mazzola 1971; Belkebir and Anglada, 1985) and *Reticulofenestra cisnerosii* (biozone NN12: Mansouri, 2021), and to the upper Zanclean based on *Globorotalia puncticulata* and *Discoaster asymmetricus* (Osman *et al*., 2021).

Biostratigraphy suggests a basal Zanclean age for the lowermost Dahra white marly limestones (*i.e.*: FO of *G. margaritae* at 5.08 Ma and LO of *R. cisnerosii* at 5.119 Ma, *i.e.,* the upper NN12 biozone, knowing that the appearance of *G. margaritae* is reported before 5.08 Ma: Fig. 3). On their western extension, these white marly limestones yielded, at their base, *Globorotalia puncticulata* associated with *Discoaster asymmetricus* (Osman *et al*., 2021) corresponding respectively to N19 and NN14/15 biozones. These biochronostratigraphic results imply that the CWML of Ouled Slama are older than those registered in the Ouled Maallah, suggesting a chronological relay of coral bioconstructions.

Consequently, these bioconstructions would have started before 5.119 Ma and disappeared a little before 3.60 Ma. Furthermore, the presence of corals like *Ceratotrochus (Edwardsotrochus) pentaradiatus* in the whitish marls (Sidi Brahim Telegraph section: Fig. 7, S4), collected between the *G. puncticulata* biozone and until before the *G. crotonensis* presence (Mazzola, 1971), suggests a degradation of this type of coral environment during the upper Zanclean as observed in the Ouled Maallah and Ouled Slama localities (Figs. 4, 5 and 6).

The abundance of *Megerlia truncata* (brachiopod) may indicate depths down to 100 m or more (Emig, 1988); its alternating abundance between the coral banks means some variations of bathymetry during the Lower Pliocene, oscillations which would probably be linked to readjustment of the margin in relation with coastal reliefs. Similarly, the species *Neopycnodonte cochlear* can affectionate this depth (up to about 50 m) in temperate waters with low turbidity (Ben Moussa, 1994). Like their modern Mediterranean representatives, these coral biobuilders seem to require, during the Lower Pliocene, a warm environment for their development, the conditions of which began to deteriorate since the disappearance of *Globorotalia puncticulata* in relation with the onset of a shallow environment. Indeed, TSB levels 32 to 49 yielded a diversified ostracofauna with a rich representation of *Aurila, Loxoconcha*, *Cytheropteron*, *Cytherella*, among others. This implies the presence of a coastal euhaline environment where frequency of planktonic forami-

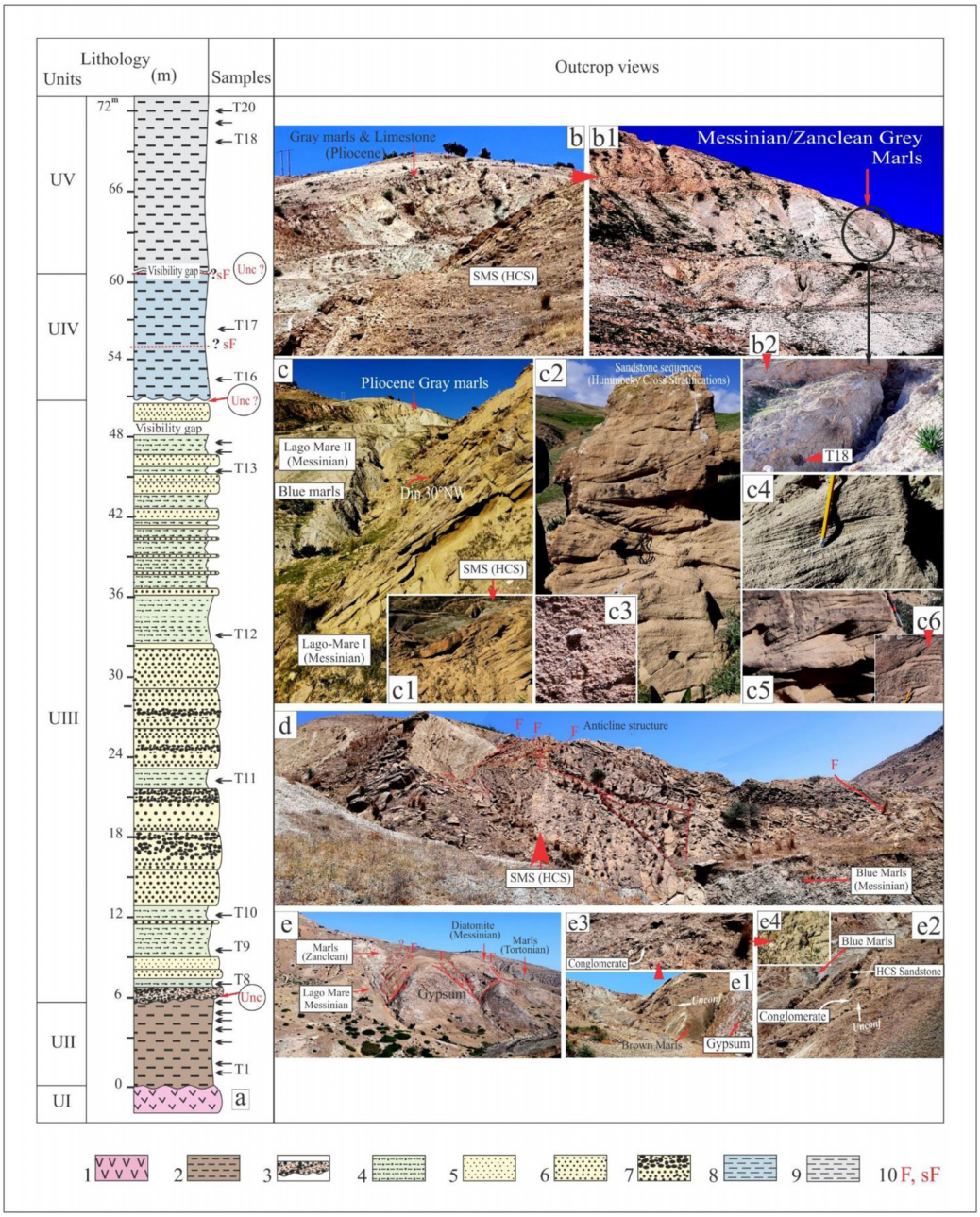

Fig. 6. Geological section of Oued Tarhia (Dahra). – Lithostratigraphic succession. 1: Selenite and anhydrite gypsum; 2: Grey to brown silt; 3: Conglomerate and sandstone; 4: Sandy clay; 5: Sandstone; 6: Coarse sandstone; 7: Sandstone, microconglomerate and conglomerate; 8: Blue marls; 9: Grey marls; 10: Fault, supposed fault. a: Log section showing lithostratigraphic of succession and sampled level position from the bottom to the top. b: View of the upper part of the Oued Tarhia section showing the Pliocene alternation of grey marl and limestone (south facade). See the dip gap existing between the beds of these deposits and the Messinian sandy marl and sandstone alternation. b: The lowest levels of Pliocene grey marls (Messinian/Zanclean boundary), the black circle indicates the location of the samples. b1: Detail showing the sampling of grey marls in a deep gully. c: The foreground shows the sandy marl and Sandstone (SMS) alternation belonging to the Messinian Lago Mare 1 (biofacies 1) ; The Pliocene gray marls appear in the background; in the center are blue marls brought back to the Messinian Lago Mare 3 (biofacies 2). c1: Detail in the sandstone benches showing a hummocky cross stratification (HCS) located under the blue marls. c2: Sandstone showing successive sedimentary structures (HCS, megaripple, oblique stratification). c3: Sorting of quartz elements marking some sandstone benches. c4: HCS. c5: Oblique stratifications. c6: Sandstone grading (coarse sandstone with microconglomerates). d: Panoramic view of the sandy marls and sandstone (SMS) alternation corresponding to the Messinian Lago Mare I (biofacies 1) capped by Messinian blue marls in the foreground; see anticline and imbricate structures (red lines), faults. e: Panoramic view showing Tortonian to Messinian lithostratigraphic units of Oued Tarhia; red lines indicate effective or suspected fault structures. e1: Unconformable succession of gypsum and grey brown clays to sandy clays and sandstone units. e2: Unconformable contact (conglomerates) between stratigraphic units (SMS and grey brown clays). e3, e4: Details of the lithostratigraphic unconformity.

Fig. 6. Coupe de l'Oued Tarhia.

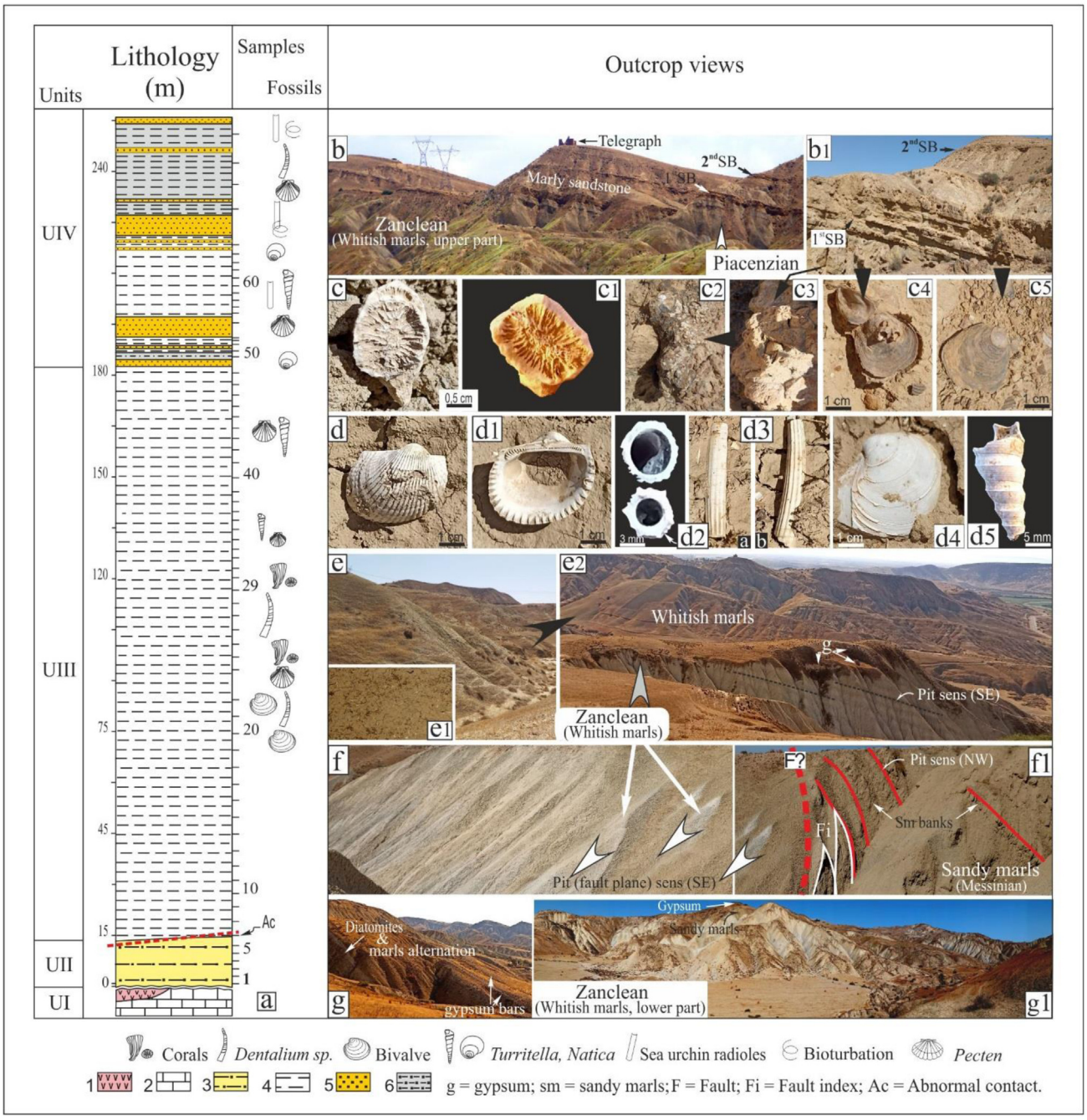

Fig. 7. Geological succession of the Sidi Brahim Telegraph section. Lithostratigraphic succession: 1: Gypsum; 2: Calcareous gypsum; 3: Sandy marls; 4: Blue (Whitish) marls; 5: Blue marls; 6: Sandstone; 7: Grey sandy marls. a: Lithology, samples and paleontological indications of the SBT geological section; b: Panoramic view showing the lithologic succession of the upper blue (whitish) marls (Zanclean) to the sandy marls and sandstone alternation (Piacenzian); b1: 1st and 2nd Sandstone bars (SB); c and c1: Scleractinian corals (*Ceratotrochus (Edwardsotrochus) pentaradiatus*); c2 and c3: Sandstone fossil concentration. c4 and c5: Ostreid shells of *Hyotissa hyotis*, fragments of Pectinids, colony of *Balanus* sp.; d and d1: *Anadara diluvii* shells. d and d3 (a,b): test of *Dentalia* sp. d4: Veneridae (*Pelecyora* sp.); d5: *Turritella* sp. Note that fossils of figures c, c1, d, d1, d2, d3, d4 and d5 are of Zanclean age. e and e1: Blue (whitsh) marls with dentals. e2: Panoramic view of the Blue (whitish) Zanclean marls: see gravity deposit (g: gypsum blocks), SE dip of the marl levels; f: Fault plane on marl sediments: see Blue (whitish) marl trails (white arrows) indicating fault plane pit; f1: Red lines indicate the plane of the sandy marl (sm) banks, broken line indicates hypothetic fault; g: Latest Messinian deposits (diatomite and marl alternation, gypsum); g1: Panoramic view showing the lower part of the Pliocene blue (whitish) marls.

Fig. 7. Coupe du Télégraphe de Sidi Brahim.

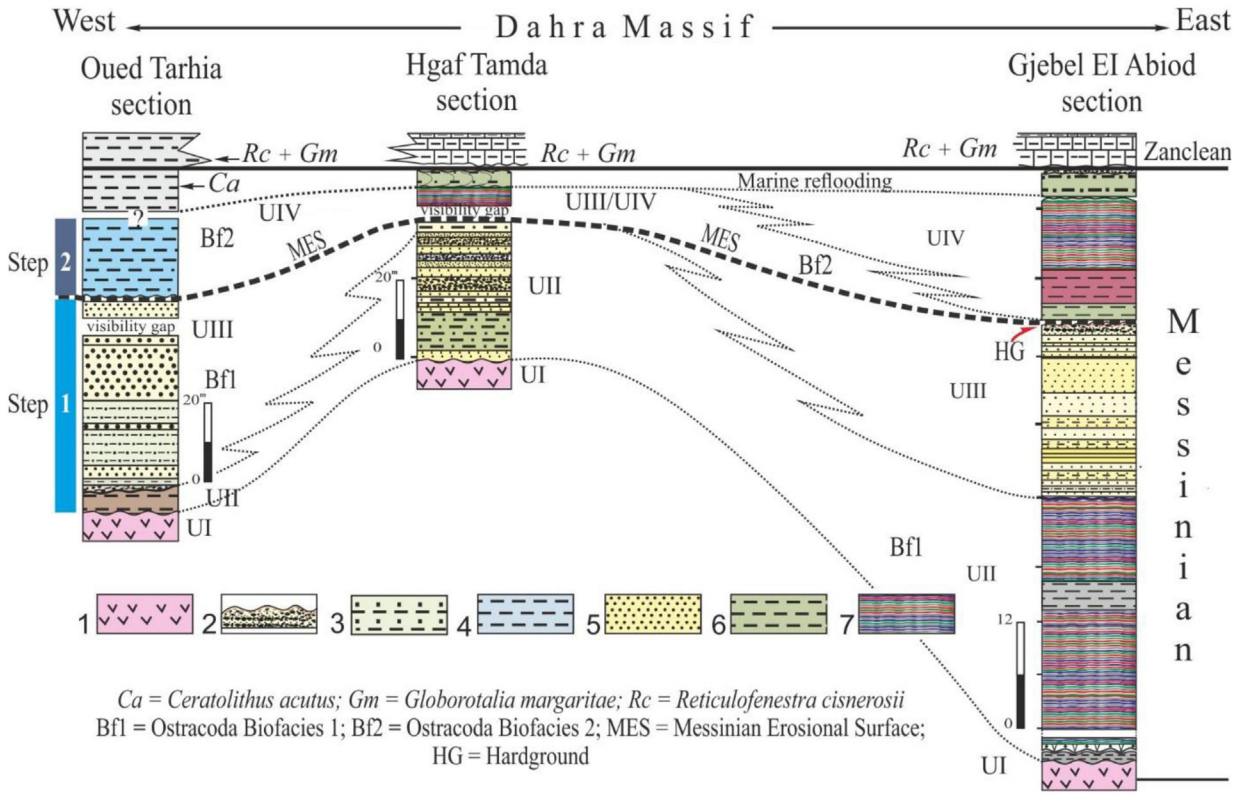

Fig. 8. Correlations of the Ouled Slama lithostratigraphic units (Djebel El Abiod, Hgaf Tamda, Oued Tarhia) and their lateral extension in the southern Dahra Massif margin. 1: Gypsum; 2: Sandstones and black shales; 3: Sandy marls; 4: Blue marls; 5: Sandstones and sandy marls; 6: Green marls; 7: Variegated and laminitic clays (varves).
Fig. 8. Corrélation des unités lithostratigraphiques des Ouled Slama et leur extension sur la marge sud du massif du Dahra.

nifera is low (levels TSB 30 to 37) to the benefit of benthic species (*Ammonia* sp, *Bulimina* sp, *Elphidium* sp.).

4.3 Dating of the Messinian-Pliocene succession in the Dahra Massif

The Sidi Brahim Telegraph section (S4; Fig. 7) is the reference section for the Lower and Upper Pliocene in the Dahra Massif. The analysis reveals the presence of several paleontological features and/or bioevents; *Globorotalia margaritae* species collected in the grey marls (TSB03 and TSB04), followed by *Ceratolithus acutus* (TSB09, associated with *G. margaritae*) in the white blue marls and *Reticulofenestra cisnerosii* (TSB11, associated with *G. margaritae* and *C. acutus*). This succession is also listed in the Oued Tarhia section (grey marine marls: T20. Fig. 6). The underlying grey marls are characterized there by an abundant ostracofauna dominated by *L. djafarovi,* (assemblage 2), attributed to the Lago Mare (Rouchy *et al*., 2007), which belongs to the late Messinian (Gliozzi, *pers. com.*). The absence of the upper part of the sandy marl and sandstone alternation is observed, the conglomerates and the hardground overlying the sediments with the ostracod assemblage 1; that demonstrates the importance of the stratigraphic gap in some localities (Oued Tarhia section), a phenomenon linked to erosion.

G. margaritae indicates the N18 biozone (Mazzola, 1971; Belkebir and Anglada, 1985; Belhadji *et al*., 2008), of Zanclean age (samples TSB3 and TSB4). The succession of *G. margaritae* and *Ceratolithus acutus*, before the appearance of *Reticulofenestra cisnerosii*, suggests a latest Messinian age for these sediments (Popescu *et al.,* 2017; Mansouri, 2021).

The sample TSB11 (blue whitish marls) reveals the presence of *G. margaritae*, *C. acutus* and *R. cisnerosii*, indicating the base of Zanclean (N18 biozone of Blow, 1969/ biozone NN12 of Martini, 1971). The Messinian-Zanclean boundary, dated at 5.33 Ma, corresponds to the FAD of *R. cisnerosii* (Mazzola, 1971; Belkebir and Anglada, 1985; Backman *et al*., 2012; Popescu *et al.*, 2017; Osman *et al*., 2021; Mansouri, 2021). It thus dates the marine reflooding before the early Zanclean (*R. cisnerosii* occurrence) (Mansouri, 2021; Cavazza and De Celles, 1998; Londeix *et al*., 2007; Carnevale *et al*., 2008; Bache *et al*., 2012; Do Couto *et al*., 2014; Clauzon *et al.,* 2015; Suc *et al*., 2015; Popescu *et al*., 2021; Van Dijk *et al*., 2023).

The appearance of *C. acutus* followed by *C. rugosus* both associated with *G. margaritae,* evidences the lower Zanclean (level TSB 17), that corresponds to biozones N18 (Mazzola, 1971; Belkebir and Anglada, 1985) and NN13 (Martini, 1971; Backman *et al*., 2012; Tchouar, 2013; Osman *et al*., 2021; Mansouri, 2021). The occurrence of *Globorotalia puncticulata* associated with *Discoaster asymmetricus*, collected in the

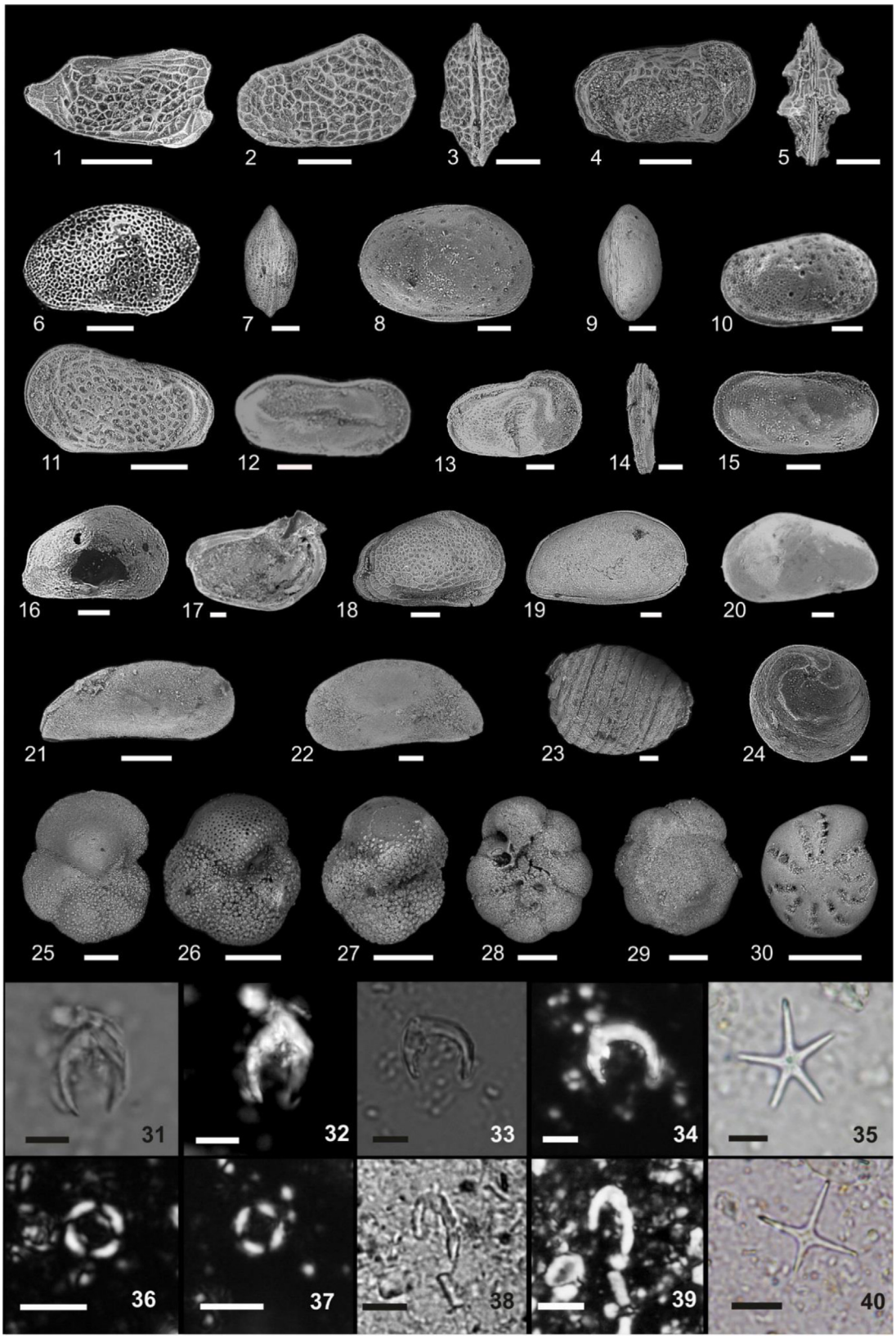
1
2
3
4
5
6
7
8
9
10
11
12
13
14
15
16
17
18
19
20
21
22
23
24
25
26
27
28
29
30
31
32
33
34
35
36
37
38
39
40

Plate 1. : Uppermost Messinian-Piacenzian microfossils from the Dahra geological succession (Lower Chelif Basin, Algeria). (Scale bar: Figs. 1-30: 100 μm; Figs. 31-40: 5 μm). Fig. 1 *Cytherura pyrama* Schneider. Carapace in left lateral view. Djebel El Abiod section (sample: Ab 23). Figs. 2-3 *Loxocornicullina djafarovi* Schneider. Carapace, 2: right lateral view; 3: dorsal view. Djebel El Abiod section (sample: Ab 23). Figs. 4-5 *Euxinocythere (Maeotocytyhere) praebaquana* Livental. Carapace, 4: left lateral view; 5: dorsal view. Djebel El Abiod section (sample: Ab 23). Figs. 6-7 *Loxoconcha* sp.1. Carapace, 6: external view; 7: dorsal view. Oued Tarhia section (sample: T17). Figs. 8-9-10 *Loxoconcha muelleri* Mehes. 8: female carapace in right lateral view. Oued Tarhia section (sample: T16). 9: female carapace in ventral view. Oued Tarhia section (sample: T17); 10: male carapace in right lateral view. Oued Tarhia section (sample: T17). Fig. 11 *Amnicythere* cf. *accicularia* Olteanu, Bonaduce and Sgarrella. Carapace in right lateral view. Djebel El Abiod section (sample: Ab 23). Figs. 12-13 *Amnicythere propinqua* Livental and Gliozzi. Carapace, 12: male carapace in left lateral view. Oued Tarhia section (sample: T17) ; 13: female carapace in right lateral view. Oued Tarhia section (sample: T16). Figs. 14-15 *Amnicythere sp.* Carapace, 14: left lateral view; 15: dorsal view. Oued Tarhia section (sample: T16). Fig. 16-17 *Tyrrhenocythere* cf. *ruggierii* Devoto. 16: juvenile right valve in lateral view; 17: juvenile right valve in internal view. Oued Tarhia section (sample: T16). Fig. 18 *Tyrrhenocythere pontica* Livental. Juvenile carapace in right lateral view. Oued Tarhia section (sample: T17). Figs. 19-20 *Cyprideis* cf. *anlavauxensis* Carbonnel.19: male carapace in right lateral view; 20: juvenile left male valve in lateral view. Oued Tarhia section (sample: T17). Fig. 21 *Zalanyiella venusta* Zalányi. Carapace in right lateral view. Djebel El Abiod section (sample: Ab 23). Fig. 22 *Camptocypria* sp. Juvenile carapace in left lateral view. Djebel El Abiod section (sample: Ab 23). Figs. 23-24 *Chara* cf.*? hispida*. 23: lateral view. Oued Tarhia section (sample: T17); 24: basal view. Oued Tarhia section (sample: T16). Fig. 25 *Globorotalia margaritae* Bolli & Bermudez. Umbilical view. Djebel El Abiod section (sample: Ab 30). Fig. 26 *Globorotalia puncticulata* Deshayes.Umbilical view. Djebel El Abiod section (sample: Ab 36). Fig. 27 *Globorotalia* cf. *crotonensis* Conato & Follador. Umbilical view. Hgaf Tamda section (sample: Ht 17). Figs. 28-29 *Ammonia* cf. *tepida* Cushman. 28: umbilical view, 29: spiral view. Djebel El Abiod section (sample: Ab 5). Fig. 30 *Elphidium sp*. Lateral view. Djebel El Abiod section (sample: Ab 8). Figs. 31-32 *Ceratolithus acutus* Gartner and Bukry. Sidi Brahim Telegraph section (sample 9; fig. 32: Polarized Light). Figs. 33-34 *Ceratolithus armatus* Müller. Sidi Brahim Telegraph section (sample 17; fig. 34: Polarized Light). Fig. 35 *Discoaster asymmetricus* Gartner. Sidi Brahim Telegraph section (sample 34). Fig. 36 *Reticulofenestra cisnerosii* Lancis and Flores. Sidi Brahim Telegraph section (sample 13; Polarized Light). Fig. 37 *Reticulofenestra cisnerosii* Lancis & Flores. Sidi Brahim Telegraph section (sample 10; Polarized Light). Figs. 38-39 *Ceratolithus rugosus* Bukry and Bramlette. Sidi Brahim Telegraph section (sample 17; fig. 39: Polarized Light). Fig. 40 *Discoaster tamalis* Kamptner. Sidi Brahim Telegraph section (sample 40).
Plate 1. Microfossiles du Messinien terminal au Plaisancien de la série du massif du Dahra.

white marls of the Sidi Brahim Telegraph section (TSB23; Fig. 7), indicates the upper Zanclean (Fig. 9).

Occurrence of *G. puncticulata* associated with *G. puncticulata* cf. *padana, Discoaster asymmetricus, D. tamalis* and *Aurila* cf. *convexa emathiae* in the TSB29 sample allows attributing this part of the whitish marls to the upper Zanclean (biozones N19-NN14/NN15). The species *Aurila* cf. *convexa emathiae* (ostracod) constitutes, according to Carbonnel and Ballesio (1982), a biozone equivalent to the *G. puncticulata* biozone (Uliczny, 1969; Sissingh, 1972, 1976).

This attribution is also valid for levels TSB30 to TSB34, some of which (TSB32-34) are marked by the presence of *G. puncticulata* cf. *padana*. In particular, the species *D. asymmetricus* and *D. tamalis* persisted there (TSB41-49). The presence of the species *Globorotalia crotonensis* (Mazzola, 1971) in the sandy marls of the Sidi Brahim Telegraph section (equivalent to level TSB51) marks the Piacenzian Stage. However, this last species may be absent in some localities of the Lower Chelif Basin; it is replaced by *G. crassaformis* (Belkebir, 1986; Belkebir and Anglada, 1985) or *G.* cf. *crassaformis* (Osman *et al*., 2021) or even *G. hirsuta aemiliana* (Belhadji *et al*., 2008).

The presence of *Discoaster tamalis* and the disappearance of Sphenoliths (*Sphenolithus abies*, among others) in the TSB66 level confirm the Piacenzian age of the Sidi Brahim Telegraph section (Mansouri, 2021). The latter section thus corresponds to a stratigraphic extension going from the late Messinian to the Piacenzian (Figs. 2 and 8) (biozones N18-N19-N20 of Blow, 1969 corresponding to biozones NN12-NN13-NN14/NN15-NN16 of Martini, 1971).

The CWML (Hgaf Tamda section) revealed the presence of five successive species. The Hg10 sample yields *G. margaritae* associated with *R. cisnerosii*. This succession indicates the N18 (Blow, 1969)/NN12 (Martini, 1971; Backman *et al*., 2012) biozones. The latter can be attributed to the basal Zanclean (Fig. 2). The Hg14 and Hg15 levels recorded *G. margaritae* associated with *G. puncticulata* indicating the N19 biozone of Blow (1969), attributed to the middle to upper Zanclean (Mazzola, 1971; Belkebir and Anglada, 1985). The species *G. puncticulata* associated with *G. bononiensis* and *G.* cf. *crotonensis* are recorded in the samples Hg16 and Hg17, indicating the N20 biozone of Blow (1969) of Piacenzian age (Fig. 10).

G. margaritae occurs in the Djebel El Abiod section; in the CWML (Ab30, Ab31), this species is associated with *R. cisnerosii* (Ab32, Ab33, Ab34, Ab35), then with *G. puncticulata* (Ab36). These bioevents assign to the CWML a Lower Pliocene age (N18 biozone of Blow, 1969 and NN12 biozone of Martini, 1971) (Fig. 10). The lower part of the overlying grey marls is attributed to the middle to upper Zanclean (biozone N19 from Blow, 1969) based on the presence of *G. margaritae* associated with *G. puncticulata* (Fig. 3). The upper part of the grey marls is assigned to the Piacenzian (biozone N20 of Blow, 1969), which yielded *G. crotonensis* over the first sandstone bar in the Djebel El Abiod section (Fig. 4: sample 49).

According to biostratigraphy, the first marine deposits of the Sidi Brahim Telegraph (*i.e.*, grey marls with *G. margaritae* and the lower part of the blue whitish marls with *C. acutus* associated with *G. margaritae*) point out the latest Messinian marine reflooding (Figs. 7 and 9). This interpretation is also valid for the grey marls of the Oued Tarhia section (Figs. 6 and 10). These data seem to confirm the observations on the bioturbated deposits from Djebel Meni-Abreuvoir and Oued El Aïcha considered as being witnesses of the restoration of

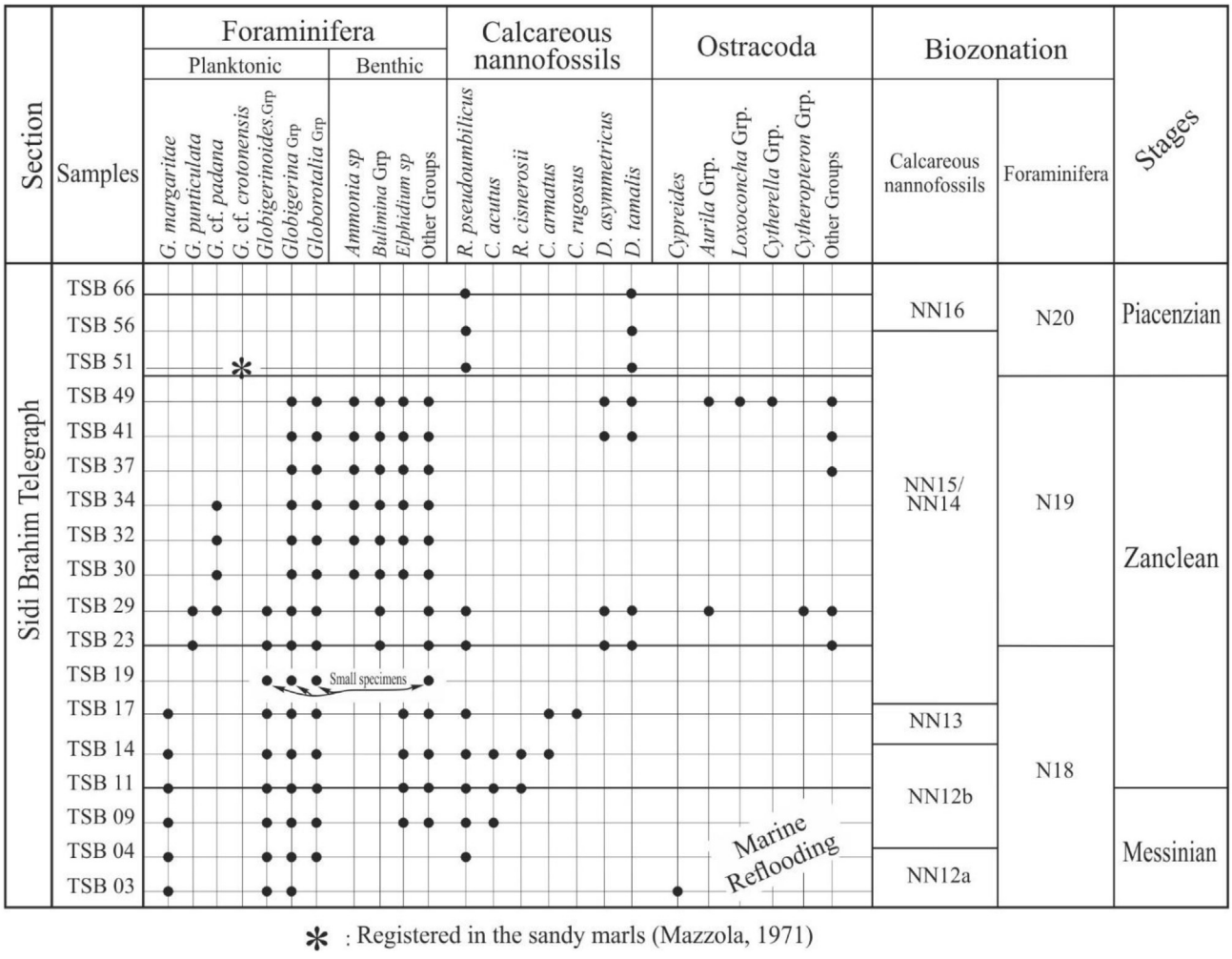

Fig. 9. Stratigraphic distribution of ostracoda, planktonic foraminifera and calcareous nannofossils from the Sidi Brahim Telegraph section
Fig. 9. Répartition stratigraphique des ostracodes, des foraminifères planctoniques et des nannofossiles calcaires dans la coupe du Télégraphe de Sidi Brahim.

marine conditions although they were ascribed to the basal Pliocene without paleontological argument (Rouchy *et al.*, 2007). These data confirm the uppermost Messinian age of the Mediterranean reflooding (Cavazza and De Celles, 1998; Londeix *et al.*, 2007; Carnevale *et al.*, 2008; Bache *et al.*, 2012; Do Couto *et al.*, 2014; Clauzon *et al.*, 2015; Suc *et al.*, 2015; Popescu *et al.*, 2021; Van Dijk *et al.*, 2023).

In addition, the Piacenzian deposits of the localities of Hgaf Tamda and Djebel El Abiod (Figs. 4, 5 and 10) underwent a significant deformation of Pliocene to Pleistocene age, having generated folds whose structural axes (syncline and anticline) are NE-SW oriented, and bounded by faults trending NS, NNE/SSW. This (transpressional) deformation is consistent with that described in the Dahra Massif (Perrodon, 1957; Arab *et al.*, 2015).

5 Discussion

Ouled Slama (Djebel El Abiod, Hgaf Tamda, Oued Tarhia), and Sidi Brahim Telegraph sections correlated with the Azaïzia one display a Miocene to Pliocene detrital sedimentation (Fig. 11), limited at the base by two beds of selenite gypsum, well known in the Lower Chelif Basin (Brive, 1897; Anderson, 1936; Perrodon 1957; Delfaud *et al.*, 1973; Rouchy, 1982a, b; Neurdin-Trescartes, 1992). This post-evaporitic sedimentation is generally ascribed to the Messinian, being of brackish or even lacustrine character or "Lago Mare" (Rouchy 1982a, b; Saint Martin, 1990; Saint Martin and Rouchy, 1990; Rouchy *et al.*, 1992, Rouchy and Caruso, 2006; Rouchy *et al.*, 2007; Atif *et al.*, 2008; Caruso *et al.*, 2020). According to a recent study at Ouled Maallah (Dahra), its stratigraphic position was correlated with other reef platforms in the Western Mediterranean (Melilla, Sorbas, etc.). The post-evaporitic deposits from Ouled Maallah are attributed to "Lago Mare 1" (Osman *et al.*, 2021).

In light of our new stratigraphic and paleontological results, we need to discuss this post-evaporitic sedimentary succession.

5.1 Assemblages 1, 2 and Lago Mare episodes in the Mediterranean region

The late Messinian (post-evaporitic) sedimentation deposits were characterized by two successive steps (step 1 aboved

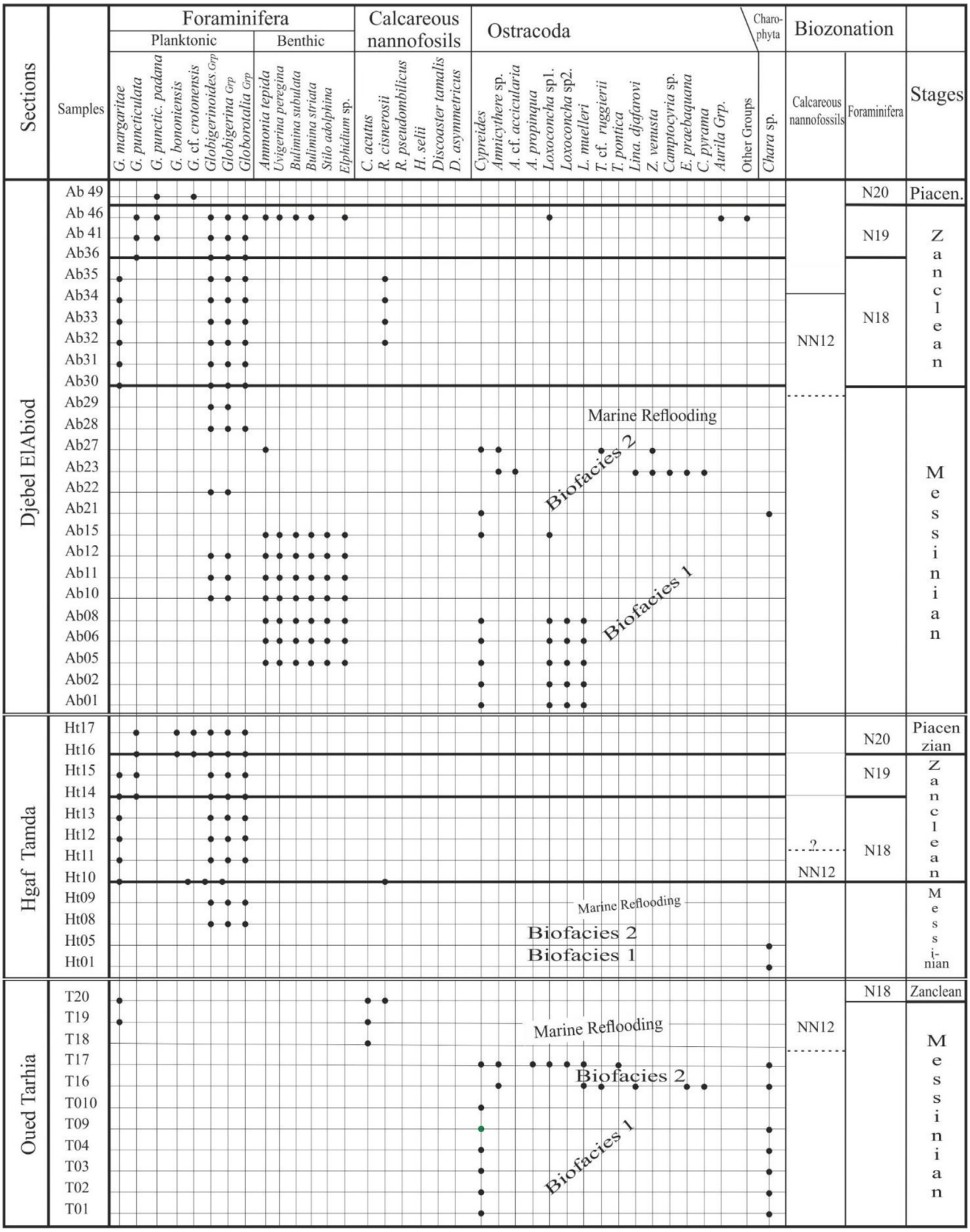

Fig. 10. Stratigraphic distribution of ostracoda, planktonic foraminifera, charophyta and calcareous nannofossils from the Ouled Slama sections (Djebel El Abiod, Hgaf Tamda, Oued Tarhia).

Fig. 10. Répartition stratigraphique des ostracodes, des foraminifères planctoniques, des charophytes et des nannofossiles calcaires dans les coupes des Ouled Slama.

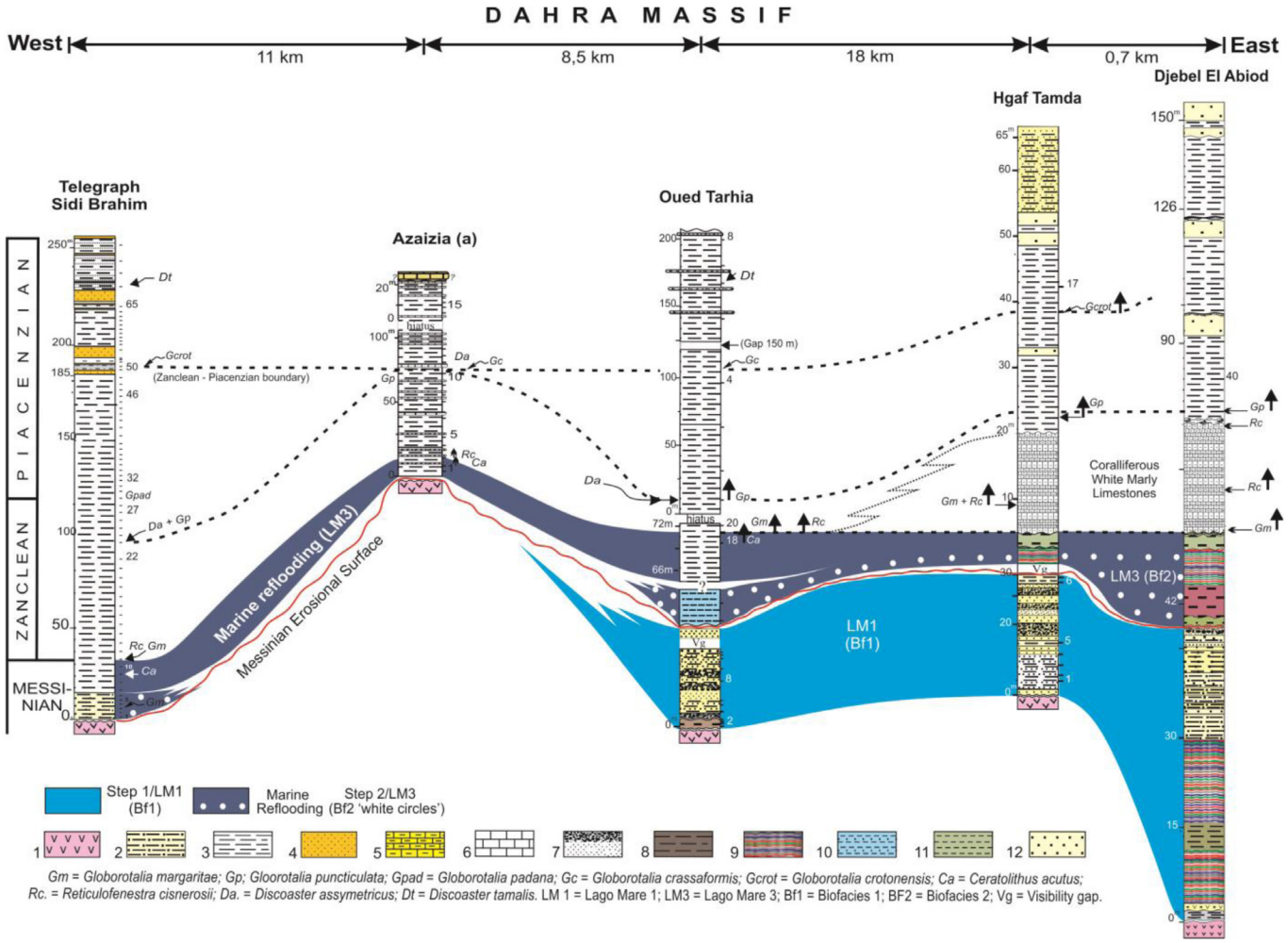

Fig. 11. Biochronology and correlations of the Ouled Slama (Oued Tarhia, Hgaf Tamda, Djebel El Abiod) and Sidi Brahim Telegraph sections correlated to the Azaïzia section: biovents, Lago Mare 1 and 3, Biofacies 1 and 2 and Messinian erosional surface (red line) from the Lower Chelif Basin.

Fig. 11. Biochronologie et corrélation des coupes des Ouled Slama, du Télégraphe de Sidi Brahim et de l'Azaïzia.

by step 2), having respectively provided two successive ostracod contents called **assemblage 1** and **assemblage 2** (Fig. 11).

The late Messinian ostracod **assemblage 1** is of Paratethyian origin (*Cyprideis*, *Loxoconcha muelleri, L.* sp.1 and *L.* sp.2) (Carbonnel and Ballesio, 1982; Gliozzi, *pers. comm.*). *Cyprideis agrigentina*, *C. anlavauxensis* associated with *Loxoconcha muelleri* and *L.* cf. *eichwaldi* (Rouchy *et al.*, 2007) complete this assemblage indicating a brackish and shallow with some episodic fluvio-lacustrine environment. Ostracod **assemblage 2** refers to the same origin and is also attributed to late Messinian (Carbonnel and Ballesio, 1982; Gliozzi and Grossi, 2008; Gliozzi, *pers. comm.*). It is dominated by *Loxocorniculina djafarovi* with *E. praebaquana*, *Amnicythere* cf. *accicularia*, *A.* sp., *Cytherura pyrama*, *Camptocypria* sp., *Zalanyiella venusta* (Pl. 1). It is followed by another assemblage of abundant *Cyprideis* with *Tyrrhenocythere* cf. *ruggierii*, *Amnicythere* sp., *Zalanyiella venusta* (see S2) of open shallow marine to brackish (*L. djafarovi*) or to slightly lacustrine (*Cyprideis* abundant) conditions.

These **assemblages** (**1** and **2:** Fig. 11) are comparable to those known in the late Messinian in the Mediterranean region. They indicate the "Lago Mare" biofacies (Bonaduce and Sgarrella, 1999; Iaccarino and Bossio, 1999; Gliozzi, 1999, Gliozzi *et al.*, 2006, 2007; Rouchy and Caruso, 2006; Gennari *et al.*, 2008; Guerra-Merchán *et al.*, 2010; Grossi *et al.*, 2015; Stoica *et al.*, 2016; Mas and Fornós, 2020). The assemblage **1** of *Cyprideis* associated with *L. muelleri* is comparable to the biofacies 1 of Bonaduce and Sgarrella (1999) where *Cyprideis* is associated with *Tyrrhenocythere ruggierii*, *Loxoconcha kochi*, *Loxoconcha muelleri* and *Caspiocypris alta* (Iaccarino and Bossio, 1999). **Assemblage 2** would correspond to biofacies 2 of Bonaduce and Sgarrella (1999), characterized by *L. djafarovi* associated with *Amnicythere*, *Loxoconcha*, *Loxocauda*, *Cytheromorpha*, *Cyprinotus* and *Tyrrhenhocythere*. Moreover, this shows that **assemblages 1** and **2** of the Dahra Massif are approximately consistent with the Apennine geological formations **p-ev1** and **p-ev2** where the species *L. djafarovi* appears, according to Roveri *et al.*, (2008), near the **p-ev1/p-ev2** boundary.

The **assemblage 1** of *Cyprideis* associated with *L. muelleri* and followed by that (**assemblage 2**) of *L. djafarovi* constitutes, like those well known in the Mediterranean, a chronological landmark sequence in the Lower Chelif Basin and the Dahra Massif. These assemblages are respectively correlated to Lago Mare biofacies 1 and Lago Mare biofacies 2 whose age is estimated between 5.59 and 5.40 Ma for the first and between 5.40 and 5.33 Ma for the second (Roveri *et al*., 2008; Grossi *et al*., 2008; Andreetto *et al*., 2022). The Lago Mare 1 of Clauzon *et al.* (2005) and Bache *et al*. (2012) is estimated between 5.64 and 5.60 Ma. It is almost coeval with Lago Mare biofacies 1 (see above). The LM3 corresponds to the post MSC marine reflooding according to Bache *et al*. (2012, 2015) and Popescu *et al*. (2017), estimated between 5.460 and 5.332 Ma (Clauzon *et al*., 2005; Popescu *et al*., 2007, 2009, 2015; Do Couto *et al*., 2014; Bache *et al*., 2012: Fig. 15). Finally, its age is slightly comparable to that recognized for Lago Mare biofacies 2 (5.40 and 5.332 Ma: Roveri *et al*., 2014b; Gliozzi and Grossi, 2008; Grossi *et al*., 2011, 2015; Gliozzi *et al*., 2007, Gliozzi *et al*., 2012).

5.2 Messinian Erosional Surface

A major discontinuity is materialized in the Dahra Massif by the hardground. This surface is underlined by a paleontological change, separating the **assemblage 1** from the **assemblage 2**. As a consequence, we interpret this discontinuity as the Messinian Erosional Surface (MES: Fig. 11) that was already evidenced in the Lower Chelif Basin thanks to a geometrical approach (Osman *et al*., 2021), so much highlighted in many other Mediterranean basins (*e.g*., Clauzon *et al*., 1996, 2005; 2015; El Euch-El Koundi *et al*., 2009; Rubino *et al*., 2010).

5.3 Age and status of the conglomerate underlying the CWML

Because of its post-hardground position, the conglomerate level of Djebel El Abiod, which is overlain by the Pliocene Coralliferous White Marly Limestone (CWML with *Reticulofenestra cisnerosii*), is estimated to be late Messinian – early Pliocene in age. This conglomeratic deposit corresponds to a sedimentation phase slightly prior to the CWML, which itself is correlated with the whitish blue marls (equivalent to the Trubi facies) of the Sidi Brahim Telegraph section. This situation is comparable to that described in the Kalamaki section (Greece) where Pierre *et al*. (2006) note the presence of deformed microconglomerates below Zanclean Trubi limestones. In the case of Djebel El Abiod, this deposit may have a status corresponding to the missing of the *Sphaeroidinellopsis subdehiscens* biozone, commonly recognized in the Lower Chelif Basin (Mazzola, 1971; Belhadji *et al*., 2008) or possibly incomplete elsewhere (Rouchy *et al*., 2007; Osman *et al*., 2021). This interpretation is supported by the succession of *Ceratolithus acutus* and *Globorotalia margaritae* observed in the grey marls of the Oued Tarhia section, the deposition of which predates the occurrence of *R. cisnerosii.*

From these data, the stratigraphic position of the conglomerate is limited at the base by the ostracod **assemblage 2** highlighted in the Dahra massif and correlated with the late Messinian age reserved to the Lago Mare biofacies 2 (Gliozzi *et al*., 2012; Grossi *et al*., 2011; Roveri *et al*., 2008, 2014b; Andreetto *et al*., 2022), between 5.40 and 5.346 Ma. Therefore, the age of conglomerate will be more later to that of the Lago Mare 3, estimated between 5,460 and 5,332 Ma (Clauzon *et al*., 2005; Bache *et al*., 2012, Bache *et al*., 2015; Do Couto *et al*., 2014, Popescu *et al*., 2015, 2017, 2021).

5.4 Coral constructions, associated fauna, age and environment of white limestones

The post-MSC restoration of normal marine conditions in the Dahra Massif (Fig. 11) began with significant sedimentation of whitish grey marls, recorded in fairly deep areas (Sidi Brahim Telepgraph). At the same time, the shallow lateral zones are marked by development of carbonate platforms (Djebel El Abiod and Hgaf Tamda) materialized by lenticular white limestones. They are dated from the early Zanclean, according to *Globorotalia margaritae* (Mazzola 1971; Belkebir and Anglada, 1985) and *Reticulofenestra cisnerosii* (Mansouri, 2021), and to the upper Zanclean based on the occurrence of *Globorotalia puncticulata* and *Discoaster asymmetricus* (Osman *et al*., 2021).

Biostratigraphy suggests for the CWML an age going from the earliest to the late lower Zanclean. This dating suggests a chronological relay of coral bioconstructions from eastern to western Dahra. The interval between 4.04 Ma (FO of *D. asymmetricus*) and 3.60 Ma (LO of *G. puncticulata* without *G. crassaformis* or *G. crotonensis*) provides the age to the topmost CWML.

Furthermore, the presence of corals like C*eratotrochus (Edwardsotrochus) pentaradiatus* in the whitish marls (Sidi Brahim Telegraph) collected between *G. puncticulata* biozone and until before the *G. crotonensis* occurrence (Mazzola, 1971) suggests a degradation of this type of coral environment during the late Zanclean in these localities.

The builder cf. *Cladocora* cf. *caespitosa* and *Dendrophyllia* sp. are generally colonial species (Laborel and Laborel-Deguen, 1978; Zibrowius, 1980; Jiménez *et al*., 2016; Altuna and Poliseno, 2019). Their modern representatives live in the Mediterranean (*e.g*., *Cladocora caespitosa*) at shallow depth (Kersting and Linares, 2009, Kersting and Linares, 2012; Kružić and Požar-Domac, 2003; Laborel, 1961; Peirano *et al*., 1998; Kružić *et al*., 2012; Özalp and Alparslan, 2011) in a warm environment. Some others are solitary and shallow organisms (*Desmophyllum*: Altuna and Poliseno, 2019). The associated *Neopycnodonte cochlear* and *Megerlia truncata* indicate depths down to 50 m or more (Ben Moussa, 1994; Emig, 1988). Their alternating abundance (*Megerlia truncata*) between the coral banks means some bathymetrical variations during the Lower Pliocene, oscillations which would probably be linked to the readjustments of the margin in relation with the coastal reliefs.

Like their modern Mediterranean representatives, these coral builders seem to live, during the Lower Pliocene, under warm conditions, which began to deteriorate since the disappearance of *G. puncticulata* in relation with the onset of a shallow environment. The corals evidenced in the Dahra Massif are well known in the Mediterranean (*Dendrophyllia*

sp., cf. *Cladocora* cf. *caespitosa*, cf. *Desmophyllum* sp., *D.* cf. *cristagalli*, *Ceratotrochus* sp., *Ceratotrochus* (*Edwardsotrochus*) *pentaradiatus*), from the Lower Miocene up to Present (Vertino *et al.*, 2014). Their presence here during the earliest Zanclean is new, compared to what is known elsewhere in the Mediterranean: late (to latest) Zanclean from Spain and Italy (Aguirre and Jiménez, 1998; Vertino *et al.*, 2014; Spadini, 2019).

The bioconstructions (cf. *Cladocora* cf. *caespitosa*, *Dendrophyllia* sp.), highlighted in the white marly limestones with *Neopycnodonte cochlear*, attest the presence of marine conditions during the lower Zanclean, warm enough for their development. Such a context is also evidenced by the presence of Proboscidea remains in this locality (Osman *et al.,* 2021). This may correspond to the warm isotopic stage TG5 (Vidal *et al.*, 2002).

6 Conclusion

The sedimentary record of the Dahra Massif provides valuable insights into the geologic history of the Lower Chelif Basin from the Messinian to the Pliocene. The post-gypsum Messinian detrital deposits of the Ouled Slama series reflect intense erosion on the continent and are followed by the Trubi equivalent Pliocene marls or coralliferous marly limestones and sandstones, including coral constructions never described before. The sections of the Dahra Massif offer a comprehensive view of the detrital laminated deposits located between the Messinian gypsum and those of the Pliocene.

6.1 Lago Mare

Two successive steps, separated by a major discontinuity (Fig. 11), characterize this deposition. They correspond to two superimposed ostracod **assemblages 1 and 2**, respectively. The first assemblage includes *Cyprideis* and *Loxoconcha mulleri*, indicative of a brackish environment affected by episodic fluvio-lacustrine inputs. The second assemblage, characterized by *Loxocorniculina djafarovi*, suggests a fairly open shallow brackish environment becoming more brackish at the top where *Cyprideis* was abundant (Fig. 11). The **assemblage 1** corresponds to the **Lago Mare biofacies 1** (Grossi *et al.*, 2015; Roveri *et al.*, 2008), that we correlate with the **LM1** (Clauzon *et al.*, 2005; Popescu *et al.*, 2015; Bache *et al.*, 2012). The **assemblage 2** is referred to the **Lago Mare biofacies 2** (Grossi *et al.*, 2011; Roveri *et al.*, 2008), that we correlate with the **LM3** (Clauzon *et al.*, 2005; Bache *et al.*, 2012; Do Couto *et al.*, 2014; Popescu *et al.*, 2015).

6.2 Messinian Erosional Surface and post-crisis marine reflooding

A hardground allows to subdivide the late Messinian post-gypsum sediments into a lower part including the ostracod **assemblage 1** and an upper part showing the ostracod **assemblage 2.** This hardground marks of a major discontinuity, interpreted here as corresponding to the Messinian Erosional Surface (Fig. 11), previously evidenced in the Lower Chelif Basin (Osman *et al.*, 2021) and so many times widely identified around the Mediterranean Basin (*e.g.*, Clauzon *et al.*, 1996, 2005, 2015; El Euch-El Koundi *et al.*, 2009; Rubino *et al.*, 2010).

The late Messinian deposits belonging to the ostracod assemblage 2, notably the detrital sedimentation with the successive occurrence of planktonic microorganisms (*Ceratolithus acutus*, *Globorotalia margaritae*, *Reticulofenestra cisnerosii*) document a marine incursion into the Lower Chelif Basin (Fig. 11). Accordingly, these deposits represent the marine reflooding of the Mediterranean Basin, which occurrend in the latest Messinian (*e.g.*, Popescu *et al.*, 2021).

6.3 Bioevents subsequent to the Lago Mare 3

Several bioevents were successively evidenced in the Dahra Massif, sealing the late Messinian Lago Mare 3 (Fig. 11). The biostratigraphic succession is comparable to that of the Sorbas Basin and other localities in the Mediterranean region where the marine reflooding has been robustly identified (Clauzon *et al.*, 2015). *Globorotalia margaritae*, *Ceratolithus acutus* and *C. rugosus* indicating an early Zanclean age are followed by *Globorotalia puncticulata* with *Discoaster asymmetricus* (late Zanclean). Therefore, *Globorotalia crotonensis*, *G. crassaformis* or *G. aemiliana* and *D. tamalis* bioevents complete the Piacenzian Stage in the Lower Chelif Basin.

6.4 Coral constructions

Scleractinian bioconstructions (cf. *Cladocora* cf. *caespitosa*, *Dendrophyllia* sp.) are reported for the first time in the Dahra Massif in white marly limestones dated from the entire lower Zanclean. These bioconstructions testify to the existence, at that time, of warm enough conditions, therefore also favorable for Proboscidea (Osman *et al.*, 2021). This relatively warm phase may correspond to the TG5 marine isotopic stage.

Supplementary materials

S1: Lithostratigraphic, sedimentological and paleontological features of the Djebel El Abiod section (Dahra Massif).

S2: Lithostratigraphic, sedimentological and paleontological features of the Hgaf Tamda section.

S3: Lithostratigraphic, sedimentological and paleontological features of the Oued Tarhia section.

S4: Lithostratigraphic, sedimentological and paleontological feature of the Sidi Brahim Telegraph section.

The Supplementary Material is available at https://www.bsgf.fr/10.1051/bsgf/2023012/olm.

Acknowledgments. This study was performed within the framework of the doctoral training of 3rd Cycle "*Geology of Marine and Continental Environments: Integrated Stratigraphy, Chronology and Dynamics of Paleoenvironments*". This work is carried out thanks to the support of the DGRSDT. It fits into the PRFU (E04N01UN310320200001) projects of the Ministry of Higher Education and Scientific Research. Professor E. Gliozzi is thanked for her help to authenticate

our ostracod determinations and for making us aware of the ongoing revision of the Paratethyan ostracoda in progress. We acknowledge the anonymous reviewer and Dr. M.C. Melinte-Dobrinescu for their critics and suggestions, which allowed to significantly improving the mansucript. The local authorities of Mazouna and El Guettar were of great help to us in our numerous field trips. The determination of some brachiopod taxa was possible thanks to the assistance of Professors A. Ouali Mehadji and P. Moissette. The authors thank Dr. F.-Z. Bessedik for valuable assistance in the English language.

References

Abbouda M, Bouhadad Y, Benfedda A, Slimani A. 2018. Seismotectonic and seismological aspects of the Mostaganem (Western Algeria) May 22, 2014 (Mw 4.9) seismic event. Arab J Geosci 11 (57): 1–9. https://doi.org/10.1007/s12517-018-3404-y

Aguirre J, Jiménez AP. 1998. Fossil analogues of present-day *Cladocora caespitosa* coral banks: sedimentary setting, dwelling community, and taphonomy (Late Pliocene, W Mediterranean). *Coral Reefs* 17: 203–213

Altuna A, Poliseno A. 2019. Taxonomy, genetics and biodiversity of mediterranean deep-sea corals and cold-water corals. In Orejas C, Jiménez C. eds. Mediterranean Cold-Water Corals: Past, Present and Future, Coral Reefs of the World 9. Springer Nature, 14: 121–156. https://doi. org/10. 1007/978-3-319-91608-8_14

Ameur-Chehbeur A. 1992. Age accuracy of some Hipparion fossiliferous sites in Algeria. In Spitz FG, Janeau G, Gonzalez S, Aulagniern xx, eds. Ongulés/Ungulates, 91, S.F.E.P.M.–I.R.G. M., Paris: Toulouse, pp. 27–30

Anderson RVV. 1936. Geology in the coastal Atlas of western Algeria, Mem Soc Geol Amer 4–450. https://doi.org/10.1130/MEM4-p1.

Andreetto F, Mancini AM, Flecker R, Gennari R, Lewis J, Lozar F *et al.* 2022. Multi-proxy investigation of the post-evaporitic succession of the Piedmont Basin (Pollenzo section, NW Italy): A new piece in the Stage 3 puzzle of the Messinian Salinity Crisis. *Palaeogeogr Palaeoclimatol Palaeoecol* 594: 110961.

Andreetto F, Aloisi G, Raad F, Heida H, Flecker R, Agiadi K *et al.* 2021. Freshening of the Mediterranean Salt Giant: controversies and certainties around the terminal (Upper Gypsum and Lago-Mare) phases of the Messinian Salinity Crisis. *Earth Sci Rev* 216, 103577: 1–47. https://doi.org/10.1016/j.earscirev.2021.103577.

Arab M, Bracene R, Roure F, Zazoun RS, Mahjoub Y, Badji R. 2015. Source rocks and related petroleum systems of the Chelif Basin, (western Tellian domain, north Algeria). *Mar Pet Geol* 64: 363–385. https:// doi.org/10.1016/j.marpetgeo.2015.03.017.

Arambourg C. 1927. Les poissons fossiles d'Oran. Matériaux carte géol. d'Algérie. Sér 1, *Palaeontol* 6: 291.

Atif KFT, Bessedik M, Belkebir L, Mansour B, Saint Martin JP. 2008. Le passage mio-pliocène dans le bassin du Bas Chélif (Algérie). Biostratigraphie et paléoenvironnements. *Geodiversitas* 30 (1): 97–116. http://sciencepress.mnhn.fr/fr/periodiques/geodiversitas/30/1/le-passage-mio-pliocene-dans-le-bassin-du-bas-chelif-algerie-biostratigraphie-et-paleoenvironnements

Bache F, Gargani J, Suc JP, Gorini C, Rabineau M, Popescu SM *et al.* 2015. Messinian evaporite deposition during sea level rise in the Gulf of Lions (Western Mediterranean). *Mar Pet Geol* 66: 262–277. https://doi.org/10.1016/j.marpetgeo.2014.12.013.

Bache F, Popescu SM, Rabineau M, Gorini C, Suc JP, Clauzon G *et al.* 2012. A two-step process for the reflooding of the Mediterranean after the Messinian Salinity Crisis. *Basin Res* 24: 125–153. https://doi.org/10.1111/j. 1365-2117. 2011.00521.x.

Backman J, Raffi I, Rio D, Fornaciari E, Pälike H. 2012. Biozonation and biochronology of Miocene through Pleistocene calcareous nannofossils from low and middle latitudes. *Newsl Stratigr* 47(2) : 221–244. https://doi.org/10.1127/0078-0421/2012/0022.

Bassetti MA, Miculan P, Sierro FJ. 2006. Evolution of depositional environments after the end of Messinian Salinity Crisis in Nijar basin (SE Betic Cordillera). *Sediment Geol* 188-189: 279–295. https://doi.org/10.1016/j.sedgeo.2006.03.009.

Belhadji A, Belkebir L, Saint Martin JP, Mansour B, Bessedik M, Conesa G. 2008. Apports des foraminifères planctoniques à la biostratigraphie du Miocène supérieur et du Pliocène de Djebel Diss (bassin du Chélif, Algérie). *Geodiversitas* 30 (1): 79–96. http://sciencepress.mnhn.fr/fr/periodiques/geodiversitas/30/1/apports-des-foraminiferes-planctoniques-la-biostratigraphie-du-miocene-superieur-et-du-pliocene-de-djebel-diss-bassin-du-chelif-algerie

Belkebir L. 1986 Le Néogène de la bordure nord occidentale du massif de Dahra (Algérie). Biostratigraphie, paléoécologie, paléogéographie. France: Doctorat Sci, Provence University, 289 p. (umpublished).

Belkebir L, Anglada R. 1985. Le Néogène de la bordure nord-occidentale du massif du Dahra. 110è Congr. natl. Soc. savantes, Sciences 6: 279–290. *Montpellier.* https://cths.fr/ed/edition.php?id=156.

Belkebir L, Bessedik M, Ameur-Chehbeur A, Anglada R. 1996. Le Miocène des bassins nord-occidentaux d'Algérie : Biostratigraphie et eustatisme. Géologie de l'Afrique et de l'Atlantique Sud : *Actes Colloques Angers* 1994: 553–561, Edit Elf Aquitaine. –: 0181–0901. - ISBN : 2- 901026–419.

Belkebir L, Labdi A, Mansour B, Bessedik M, Saint Martin JP. 2008. Biostratigraphie et lithologie des séries serravallo-tortoniennes du massif du Dahra et du bassin du Chélif (Algérie). Implications sur la position de la limite serravallo-tortonienne. *Geodiversitas* 30 (1) : 9–19. http://sciencepress.mnhn.fr/fr/periodiques/geodiversitas/30/1/biostratigraphie-et-lithologie-des-series-serravallo-tortoniennes-du-massif-du-dahra-et-du-bassin-du-chelif-algerie-implications-sur-la-position-de-la-limite-serravallo-tortonienne

Ben Moussa A. 1994. Les bivalves néogènes du Maroc septentrional (façades atlantiques et méditerranéenne) : biostratigraphie, paléobiogéographie et paléoécologie. *Docum Lab Géol Lyon* 132: 281.

Bendella M, Benyoucef M, Mukilas R, Bouchemla I, Ferré B. 2021. Shallow to marginal marine ichnoassemblages from the Upper Pliocene Slama Formation (Lower Chelif Basin, NW Algeria). *Geol Carpathica*. http://dx.doi.org/10.31577/GeolCarp.72.4.9

Benyoucef M, Bendella M, Brunetti M, Ferré B, Koci T, Bouchemla I *et al.* 2021. Upper Pliocene bivalve shell concentrations from the Lower Chelif basin (NW Algeria): Systematics, sedimentologic and taphonomic framework. *Ann Paléontol* 107, 102509: 1–23. https://doi.org/10.1016/j.annpal.2021.102509

Bessedik M, Belkebir L, Mansour B. 2002. Révision de l'âge miocène inférieur (au sens des anciens auteurs) des dépôts du Bassin du Bas Chélif (Oran, Algérie) : conséquences biostratigraphique et géodynamique. *Mém Serv Géol Algérie* 11: 167–186.

Bessedik M, Benammi M, Jaeger JJ, Ameur-Chehbeur R, Belkebir L, Mansour B. 1997. Gisement à rongeurs d'âge tortonien dans des dépôts lagunaires et marins de transition en Oranie: corrélation marin continental. Actes du congrès BiochroM'97, In Aguilar JP, Legendre S, Michaux J. eds. Mém. Trav. EPHE, Inst. Montpellier, V 21, pp. 293–300.

Bizon G, Bizon JJ. 1972. Atlas des principaux foraminifères planctoniques du Bassin méditerranéen Oligocène à Quaternaire. *Technip* (édit.), Paris, 316 p.

Blow WH. 1969. Late Middle Eocene to Recent planctonic foraminiferal biostratigraphy. *Proc lst lnt Conf Plankt Microfossils*, Genève 1, pp. 199–422.

Bonaduce G, Sgarrella F. 1999. Paleoecological interpretation of the latest Messinian sediments from southern Sicily (Italy). *Soc Geol Ital Mem* 54: 83–91.

Brive A. 1897. La carte géologique de Renault au 1/50 000è, n° 104 et notice explicative. Edition du Service géographique de l'Armée.

Butler RWH, McClelland E, Jones RE. 1999. Calibrating the duration and timing of the Messinian salinity crisis in the Mediterranean: linked tectonoclimatic signals in thrust-top basins of Sicily. *J Geol Soc London* 156: 827–835. https://doi.org/10.1144/gsjgs.156.4.0827.

Carbonnel G, Ballesio R. 1982. Les ostracodes pliocènes du Sud-Est de la France. *Docum Lab Géol Lyon* 85: 113.

Carnevale G, Longinelli A, Caputo D, Barbieri M, Landini W. 2008. Did the Mediterranean marine reflooding precede the Mio-Pliocene boundary? Paleontological and geochemical evidence from upper Messinian sequences of Tuscany, Italy. Palaeogeogr Palaeoclimatol Palaeoecol 257: 81–105. https: //doi.org/10.1016/j.palaeo.2007.09.005.

Caruso A, Blanc-Valleron MM, Da Prato S, Pierre C, Rouchy JM. 2020. The late Messinian "lago-Mare" event and the Zanclean reflooding in the Mediterranean Sea: insights from the Cuevas del Almanzora section (Vera Basin, South-Eastern Spain). *Earth Sci Rev* 200 (102993): 1–20. https://doi.org/10.1016/j.earscirev.2019.102993.

Cavazza W, DeCelles PG. 1998. Upper Messinian siliciclastic rocks in southeastern Calabria (southern Italy): paleotectonic and eustatic implications for the evolution of the central Mediterranean region. *Tectonophysics* 298 : 223–241. https://doi.org/10.1016/S0040-1951(98) 00186-3.

Channell JET, Di Stefano E, Sprovieri R. 1992. Calcareous plankton biostratigraphy and paleoclimatic history of the Plio-Pleistocene Monte San Nicola Section (Southern Sicily). *Boll Soc Paleontol Ital* 31: 351–382.

Channell JET, Rio D, Thunell RC. 1988. Miocene/Pliocene magnetostratigraphy at Capo Spartivento, Calabria, Italy. *Geology* 16: 1096–1099. https://doi.org/10.1130/ 0091-7613 (1988) 016<1096: MPBMAC>2.3.CO; 2

Chikhi H. 1992. Une palynoflore méditerranéenne à subtropicale au Messinien pré évaporitique en Algérie. *Géol Méditer*, Marseille, 19 (1): 19–30.

CIESM. 2008. Executive summary. In: the Messinian Salinity Crisis from mega-deposits to microbiology a consensus report (Ed F. Briand). *CIESM Workshop Monographs* 33: 7–28. http://www.ciesm.org/online/monographs/Almeria.html

Cita MB. 1975. Studi sul Pliocene e egli strati di passagio dal Miocene al Pliocene. VII. Planktonic foraminiferal biozonation of the Mediterranean Pliocene deep-sea record, a revision. *Riv Ital Paleontol Stratigr* 81: 527–544.

Clauzon G, Suc JP, Do Couto D, Jouannic G, Melinte-Dobrinescu MC, Jolivet L *et al.* 2015. New insights on the Sorbas Basin (SE Spain): the onshore reference of the Messinian Salinity Crisis. *Mar Petrol Geol* 66: 71–100. https:// doi.org/10.1016/j.marpetgeo.2015.02.016.

Clauzon G, Suc JP, Gautier F, Berger A, Loutre, MF. 1996. Alternate interpretation of the Messinian salinity crisis, controversy resolved ? *Geology* 24: 363–366.

Clauzon G, Suc JP, Popescu SM, Marunteanu M, Rubino JL, Marinescu F *et al.* 2005. Influence of the Mediterranean sea-level changes over the Dacic Basin (Eastern Paratethys) in the Late Neogene. The Mediterranean Lago Mare facies deciphered. *Basin Res* 17: 437–462. https://doi.org/10.1111/j. 1365-2117.2005.00269.x.

Cornée JJ, Saint Martin JP, Conesa G, Muller J. 1994. Geometry, palaeoenvironments and relative sea level (accommodation space) changes in the Messinian Murdjadjo carbonate platform (Oran, western Algeria): consequences. *Sed Geol* 89 (1-2): 143–158. https://doi.org/10.1016/ 0037-0738 (94) 90087-6.

Cornée JJ, Saint Martin JP, Conesa G, Münch P, André JP, Saint Martin S *et al.* 2004. Correlations and sequence stratigraphic model for Messinian carbonate platforms of the western and central Mediterranean. *Int J Earth Sci (Geol Rundsch)* 93: 621–633. https://doi.org/10.1007/s00531-004- 0400-0.

Cunningham KJ, Benson RH, Rakic-El Bied K, McKenna LW. 1997. Eustatic implications of Late Miocene depositional sequences in the Melilla Basin, northeastern Morocco. *Sediment Geol* 107: 147–165. https://doi.org/10.1016/S0037-0738(96) 00037-1.

Cunningham KJ, Collins LS. 2002. Controls on facies and sequence stratigraphy of an upper Miocene carbonate ramp and platform, Melilla basin, *NE Morocco. Sediment Geol* 146 (3-4): 285–304. https://doi.org/10.1016/S0037-0738(01) 00131-2.

DeCelles PG, Cavazza W. 1995. Upper Messinian conglomerates in Calabria, southern Italy: Response to orogenic wedge adjustment following Mediterranean sea-level changes. *Geology* 23 (9): 775–778.

Delfaud J, Michaux J, Neurdin J, Revert J. 1973. Un modèle paléogéographique de la bordure méditerranéenne : évolution de la région oranaise (Algérie) au Miocène supérieur. Conséquences stratigraphiques. *Bull Soc Hist Nat Afr Nord Alger* 64: 219–241.

Derder MEM, Henry B, Maouche S, Bayou B, Amenna M, Besse J *et al.* 2013. Transpressive tectonics along a major E-W crustal structure on the Algerian continental margin: Blocks rotations revealed by a paleomagnetic analysis. *Tectonophysics* 593: 183–192. https://doi.org/10.1016/j.tecto.2013.03.007.

Di Stefano A, Sturiale G. 2010. Refinements of calcareous nannofossil biostratigraphy at the Miocene/Pliocene boundary in the Mediterranean region. *Geobios* 43: 5–20.

Do Couto D, Popescu SM, Suc JP, Melinte-Dobrinescu MC, Barhoun N, Gorini C *et al.* 2014. Lago Mare and the Messinian salinity crisis: evidence from the Alboran Sea (S. Spain). Mar Pet Geol 52: 57–76. https:// doi.org/10.1016/j.marpetgeo.2014.01.018.

El Euch-El Koundi N, Ferry S, Suc J-P., Clauzon G,Melinte-Dobrinescu MC, Gorini C *et al.* 2009. Messinian deposits and erosion in northern Tunisia: inferences on Strait of Sicily during the Messinian Salinity Crisis. *Terra Nova* 21 : 41–48.

Emig CC. 1988. Les brachiopods actuels sont-ils des indicateurs (paléo) bathymétriques. *Géologie Méditerranéenne*, vo. XV, 1: 65–71.

Esteban M. 1979. Significance of the upper miocene coral reefs of the western Mediterranean. *Palaeogeogr Palaeoclimatol Palaeoecol* 29: 169–188. https://doi.org/10.1016/ 0031-0182 (79) 90080-4.

Fenet B, Irr F. 1973. Observations sur le Pliocène inférieur et moyen de la région des Andalouses (littoral oranais, Algérie). *CR Acad Sci*, Paris, 276, D:;1; 2761–2764.

Gaudant J, Saint Martin JP, Bessedik M, Mansour B, Moissette P, Rouchy JM. 1997. Découverte d'une frayère de poissons téléostéens dans des diatomites messiniennes du Djebel Murdjadjo (environs d'Oran, Algérie). *J African Earth Sci* 24/4: 511–529. https://doi.org/10.1016/S0899-5362(97)00078-X.

Gautier F, Clauzon G, Suc JP, Cravatte J. 1994. Age et durée de la crise de salinité messinienne. *CR Acad Sci*, Paris, 318 (2): 1103–1109.

Gennari R, Iaccarino SM, Di Stefano A, Sturiale G, Cipollari P, Manzi V *et al.* 2008. The Messinian-Zanclean boundary in the Northern Apennine. *Stratigraphy.* 5., (3-4): 307–322.

Gliozzi E, Ceci ME, Grossi F, Ligios S. 2007. Paratethyan ostracod immigrants in Italy during the Late Miocene. *Geobios* 40 (3): 325–337. https://doi.org/10.1016/j. geobios.2006.10.004.

Gliozzi E, Grossi F, Cosentino D, Iadanza A. 2012. The late Messinian Lago-Mare biofacies in central Apennines: the ostracod perspective. *Soc Geol Itaniana*, Roma 23: 63–65.

Gliozzi E, Grossi F. 2008. Late Messinian lago-mare ostracod paleoecology: a correspondence analysis approach. *Paleogeogr Paleoclimatol Paleoecol* 264 (3-4): 288–295. https://doi.org/10.1016/j.paleo.2007.03.055.

Gliozzi E, Grossi, F, Cosentino D. 2006. Late Messinian biozonation in the Mediterranean area using Ostracodi: a proposal. R.C.M.N.S. *Acta Naturalia de "L'Ateneo Parmense"* 42: A. 21.

Gliozzi E. 1999. A late Messinian brackish water ostracod fauna of Paratethyan aspect from Le Vicenne Basin (Abruzzi, central Apennines, Italy). *Paleogeogr Paleoclimatol Paleoecol* 151 (1-3): 191–208.

Gradstein FM, Ogg JG, Schmitz MD, Ogg GM. 2012. The geologic time scale. Vol 1, 1st edit, Elsevier. Publisher: 413 p.

Grossi F, Cosentino D, Gliozzi E. 2008. Late Messinian Lago-Mare ostracods and paleoenvironments of the central and eastern Mediterranean Basin. *Boll Soc Paleontol Ital* 47 (2): 131–146.

Grossi F, Gliozzi E, Anadón P, Castorina F, Voltaggio M. 2015. Is *Cyprideis agrigentina*. Decima a good paleosalinometer for the Messinian Salinity Crisis? Morphometrical and geochemical analyses from the Eraclea Minoa section (Sicily). *Paleogeogr Paleoclimatol Paleoecol* 419: 75–89. https: //doi.org/10.1016/j.paleo.2014.09.024.

Grossi F, Gliozzi E, Cosentino D. 2011. Paratethyan ostracod immigrants mark the biostratigraphy of the Messinian Salinity Crisis. *Joannea Geol Paläont* 11: 66–68.

Guardia P. 1975. Géodynamique de la marge alpine du continent africain d'après l'étude de l'Oranie nord-occidentale. *Thèse Doctorat d'Etat*, Nice University.

Guardia P. 1976. Carte géologique de l'Oranie nord occidentale au 1/100 000è. CRGM: Nice University.

Guerra-Merchán A, Serrano F, Garcés M, Gofas S, Esu D, Gliozzi E *et al.* 2010. Messinian Lago-Mare deposits near the strait of Gibraltar (Malaga basin, S Spain). Paleogeogr Paleoclimatol Paleoecol 285 (3-4): 264–276. https://doi.org/ 10.1016/j.paleo.2009.11.019.

Hilgen FJ, Lourens LJ, Van Dam JA. 2012. The Neogene period. In: Gradstein *et al.* ed.,The geological Time scale 2012. 1st ed.Elsevier BV. Publisher, pp. 923–977. https://doi. org/10. 1016/j. palaeo. 2022. 110961

Iaccarino S, Bossio A. 1999. Paleoenvironment of uppermost Messinian sequences in the western Mediterranean (Sites 974, 975, and 978). In: Proceedings of the Ocean Drilling Program, Scientific Results. College Station, TX: Ocean Drilling Program, Vol. 161, pp. 529–541.

Iaccarino SM, Premoli Silva I, Biolzi M, Foresi LM, Lirer F, Turco E *et al.* 2007. Practical manual of Neogene planktonic foraminifera. Perugia: Università di Perugia Press International School on Planktonic Foraminifera, (Neogene Planktonic Foraminifera), pp. 1–180.

Jiménez C, Achilleos K, Abu Alhaija R, Gili JM, Orejas C. 2016. Living in close quarters: epibionts on *Dendrophyllia ramea* deep-water corals (Cyprus and Menorca channel). *Rapp Comm Int Mer Médit* 41: 466.

Kersting DK, Linares C. 2009. Mass mortalities of *Cladocora caespitosa* in relation to water temperature in the Columbretes Islands (NW Mediterranean). Presented in *ASLO Aquatic Sciences Meeting*, Nice, France.

Kersting DK, Linares C. 2012. *Cladocora caespitosa*. bioconstructions in the Columbretes Islands Marine Reserve (Spain, NW Mediterranean): distribution, size structure and growth. *Mar Ecol* 33: 427–436. https://doi.org/10.1111/j. 1439-0485. 2011.00508.x

Krijgsman W, Fortuin AR, Hilgen FJ, Sierro FJ. 2001. Astrochronology for the Messinian Sorbas basin (SE Spain) and orbital (precessional) forcing for evaporite cyclicity. *Sedim Geol* 140: 43–60.

Krijgsman W, Hilgen FJ, Raffi I, Sierro FJ, Wilsonk DS. 1999. Chronology, causes and progression of the Messinian salinity crisis. *Nature*, 400, Macmillan Magazines Ltd, 652–655.

Kružić P, Požar-Domac A. 2003. Banks of the coral Cladocora caespitosa (Anthozoa, Scleractinia) in the Adriatic Sea. *Coral Reefs* 22: 536. https://doi.org/10.1007/s00338-003-0345-y.

Kružić P, Sršen P, Benkovic L. 2012. The impact of seawter temperature on coral growth parameters of the colonial coral *Cladocora caespitosa* (Anthozoa, Scleratinia) in the eastern Adritic Sea. *Facies* 58: 477–491.

Laborel J, Laborel-Deguen F. 1978. Abondance du madréporaire *Cladocora caespitosa* (Linné, 1767) dans les herbiers de posidonies de la baie de Port-Cros. *Travaux scientifiques du Parc national de Port-Cros* 4: 273–274.

Laborel J. 1961. Sur un cas particulier de concrétionnement animal. Concrétionnement à *Cladocora caespitosa* (L.) dans le Golfe de Talante. *Int Explor Sci Mer* 16 (2): 429–432.

Langereis CG, Hilgen FJ. 1991. The Capo Rossello composite: a Mediterranean and global reference section for the early to early late Pliocene. Earth Planet Sci Lett 104 (2-4): 211–225. https://doi.org/10. 1016/0012-821X (91)90205-V.

Leprêtre R, de Lamotte DF, Combier V, Gimeno-Vives O, Mohn G, Eschard R. 2018. The Tell-Rif orogenic system (Morocco, Algeria, Tunisia) and the structural heritage of the southern Tethys margin. *BSGF Earth Sciences Bulletin* 189 (10): 1–35. https://doi.org/10.1051/bsgf/2018009.

Lirer F, Foresi LM, Iaccarino SM, Salvatorini G, Turco E, Cosentino C *et al.* 2019. Mediterranean Neogene planktonic foraminifer biozonation and biochronology. *Earth Sci Rev* 196 (102869): 1–36. https://doi.org/10.1016/j.earscirev.2019.05.013.

Londeix L, Benzakour M, Suc JP, Turon JL. 2007. Messinian palaeoenvironments and hydrology in Sicily (Italy): the dinoflagellate cyst record. *Geobios* 40: 233–250. https://doi.org/10.1016/j.geobios.2006.12.001.

Lourens LJ, Hilgen FJ, Shackleton NJ, Laskar J, Wilson D. 2004. The Neogene period. In Gradstein FM, Ogg JG, Smith AG eds. A geologic time scale 200. Cambridge University Press, Vol. 21, pp. 409–440.

Lourens LJ, Sluijs A, Kroon D, Zachos JC, Thomas E, Rohl U *et al.* 2005. Astronomical pacing of late Palaeocene to early Eocene global warming events. Nature 435 (23): 1083–1087. https://doi.org/10.1038/nature03814.

Mahboubi S, Bennami, M, Jaeger JJ. 2015. New datation of the Tafna Basin (Algeria): a combination between biochronological and magnetostratigraphical data. *Palaevertebrata*, Montpellier, 39(1-e1): 1–11.

Mansour B, Saint Martin JP. 1999. Conditions de dépôt des diatomites messiniennes en contexte de plateforme carbonatée d'après l'étude des assemblages de diatomées: Exemple du Djebel Murdjadjo (Algérie). *Geobios* 32 (3): 395–408. https://doi.org/10.1016/S0016-6995 (99) 80016-3.

Mansouri MEH, Bessedik M, Aubbry MP, Belkebir L, Mansour B, Beaufort L. 2008. Contribution biostratigraphiques et paléoenvironnementales de l'étude des nannofossiles calcaires des dépôts tortono messiniens du bassin du Chélif (Algérie). *Geodiversitas* 30

(1): 59–77. http://sciencepress.mnhn.fr/fr/periodiques/geodiversitas/30/1/contributions-biostratigraphiqueset-paleoenvironnementales-de-l-etudedes-nannofossiles-calcairesdes-depots-tortono-messiniens-du-bassin-du-chelif-algerie

Mansouri MEH. 2021. Les nannofossiles calcaires néogènes du Bassin du bas Chélif (systématique et biostratigraphie). *Thèse de Doctorat Sciences*, Université d'Oran 2, 206 p.

Manzi V, Gennari R, Hilgen F, Krijgsman W, Lugli S, Roveri M *et al.* 2013. Age refinement of the Messinian salinity crisis onset in the Mediterranean. *Terra Nova*, 25, 4: 315–322. https://doi.org/10.1111/ter.12038.

Manzi V, Lugli S, Roveri M, Schreiber BC. 2009. A new facies model for the Upper Gypsum of Sicily (Italy): chronological and paleoenvironmental constraits for the Messinian salinity crisis in the Mediterranean. *Sedimentology* 56: 1937–1960. https://doi.org/10.1111/j. 1365-3091. 2009.01063.x.

Martini E. 1971. Standard Tertiary and Quaternary calcareous nannoplankton zonation. Proceedings of the *2nd Planktonic Conference* Roma, Vol. 2, pp. 739–785

Mas G, Fornós JJ. 2020. The messinian salinity crisis in Mallorca: new insights for a western mediterranean stratigraphic scenario. *Mar Pet Geol* 104656. https://doi. org/10.1016/j.marpetgeo.2020.104656.

Mazzola C. 1971. Les foraminifères planctoniques du Mio-Pliocène de l'Algérie nord-occidentale. *Proceeding on the Snd International Conference on the Planktonic Microfossils*, Roma, 2: 787–818.

Meghraoui M, Cisternas A, Philip H. 1986. Seismotectonic of the Lower Cheliff Basin: Structural background of the El Asnam (Algeria) Earthquake. *Tectonics* 5, 6: 809–836. https://doi.org/10.1029/TC005i006p00809.

Meghraoui M, Philip H, Albarède F, Cisternas A. 1988. Trenches investigations through the trace of the 1980 El-Asnam thrust fault: evidence for paleoseismicity. *Bull Seismol Soc Amer* 78 (2): 979–999. https://www.researchgate.net/publication/281263571.

Meghraoui M. 1982. Etude néotectonique de la région nord-est d'El-Asnam: relation avec le séisme du 10 octobre 1980. *3th cycle thesis*, Paris7 Univ. , pp. 210.

Moulana ML, Hubert-Ferrari A, Guendouz M, Doutreloup S, Roubinet S, Collignon B *et al.* 2022. Karstic geomorphology of Carbonate Ouarsenis Piedmont (Boukadir Region, Chelif) in Algeria: the role of the Messinian Salinity Crisis. *J African Earth Sci*. https://doi.org/10.1016/j.jafrearsci.2022.104697.

Moulana ML, Hubert-Ferrari A, Guendouz M, El Ouahabi M, Boutaleb A, Boulvain F. 2021. Contribution to the sedimentology of the Messinian carbonates of the Chelif Basin (Boukadir, Algeria). *Geol Bel* 24/1-2: 85–104.

Neurdin-Trescartes J. 1992. Le remplissage sédimentaire du bassin néogène du Chélif, modèle de référence de bassins intramontagneux. *Thèse doctorat d'état*, Université de Pau & Pays de l'Adour, 1, 332 p.

Neurdin-Trescartes J. 1995. Paléogéographie du Bassin du Chélif (Algérie) au Miocène. Causes et conséquences. *Géol Méditer* 22 (2): 61–71.

Orszag-Sperber F. 2006. Changing perspectives in the concept of "Lago-Mare" in Mediterranean Late Miocene evolution. *Sediment Geol* 188 (189): 259–277. https://doi.org/10.1016/j.sedgeo.2006.03.008.

Orszag-Sperber F, Rouchy JM, Blanc-Valleron M. 2000. La transition Messinien-Pliocène en Méditerranée orientale (Chypre) : la période du Lago-Mare et sa signification. Comptes Rendus de l'Académie des Sciences Paris, *Sci Terre et Planètes* 331: 483–490. https://doi.org/10.1016/S1251-8050(00) 01433-6.

Osman MK, Bessedik M, Belkebir L, Mansouri MEH, Atik A, Belkhir A *et al.* 2021. Messinian to Piacenzian deposits, erosion, and subsequent marine bioevents in the Dahra Massif (Lower Chelif Basin, Algeria). *Arab J Geosci* 14, 684: 1–36. https://doi.org/10.1007/s12517-021- 06481-0.

Ouda K, Ameur A. 1978. Contribution of the biostratigraphy of the Miocene sediments associated with primitive *Hipparion* fauna of Bouhanifia, North West Africa. *Revista Española Micropaleontol* 10 (3): 407–420.

Özalp HB, Alparslan M. 2011. The First Record of *Cladocora caespitosa* (Linnaeus, 1767) (Anthozoa, Scleractinia) from the Marmara Sea. *Turkish J Zool* 35: 701–705.

Peirano A, Morri C, Mastronuzzi G, Bianchi CN. 1998. The coral *Cladocora caespitosa* (Anthozoa, Scleractinia) as a bioherm builder in the Mediterranean Sea. *Mem Descr Carta Geol Ital* 52 (1994) 59–74.

Pellen R, Popescu SM, Suc JP, Melinte-Dobrinescu MC, Rubino JL, Rabineau M *et al.* 2017. The Apennine foredeep (Italy) during the latest Messinian: Lago Mare reflects competing brackish and marine conditions based on calcareous nannofossils and dinoflagellate cysts. ,*Geobios* 50 (3): 237–257.

Perrodon A. 1957. Etude géologique des bassins néogènes sublittoraux de l'Algérie occidentale. *Bulletin du Service de la Carte Géologique de l'Algérie*, Alger, 12: 1–382.

Pierre C, Caruso A, Blanc-Valleron MM, Rouchy JM, OrszagSperber F. 2006. Reconstruction of the paleoenvironmental changes around the Messinian-Pliocene boundary along a West-East transect across the Mediterranean. *Sediment Geol* 188/189: 319–340.

Pomel A. 1892. Sur la classification des terrains miocènes de l'Algérie et réponses aux critiques de M. Peron. *Bull Soc géol Fr* 96, sér 3, 20: 166–174.

Popescu SM, Cavazza W, Suc JP, Melinte-Dobrinescu MC, Barhoun N, Gorini C. 2021. Pre-Zanclean end of the Messinian Salinity Crisis: new evidence from central Mediterranean reference sections. *J Geol Soc*. https://doi.org/10.1144/jgs 2020-183.

Popescu SM, Dalibard M, Suc JP, Barhoun N, Melinte-Dobrinescu MC, Bassetti MA *et al.* 2015. Lago Mare episodes around the Messinian-Zanclean boundary in the deep southwestern Mediterranean. *Mar Pet Geol* 66: 55–70. https://doi.org/10.1016/j.marpetgeo.2015.04.002.

Popescu SM, Melinte-Dobrinescu MC, Suc JP, Clauzon G, Quillévére F, Suto-Szentai M. 2007. Earliest Zanclean age for the Colombacci and uppermost Di Tetto formations of the "latest Messinian" northern Apennines: New palaeoenvironmental data from the Maccarone section (Marche Province, Italy). *Geobios* 40: 359–373. https://doi.org/10.1016/j.geobios.2006.11.005.

Popescu SM, Melinte-Dobrinescu MC, Suc JP, Do Couto F D. 2017. Ceratolithus acutus Gartner and Bukry 1974 (=C. armatus Müller 1974), calcareous nannofossil marker of the marine reflooding that terminated the Messinian salinity crisis: Comment on "Paratethyan ostracods in the Spanish Lago-Mare: More evidence for interbasinal exchange at high Mediterranean sea level" by Stoica et al., 2016. *Palaeogeogr Palaeoclimatol Palaeoecol* 441: 854–870. Palaeogeogr Palaeoclimatol Palaeoecol 485: 986-989. https://doi.org/10.1016/j.palaeo.2016.07.011.

Popescu SM, Melinte-Dobrinescu MC, Dalesme F, Sütö-Szentai M, Jouannic G, Bakrac K *et al.* 2009. Galeacysta etrusca complex, dinoflagellate cyst marker of Paratethyan influxes into the Mediterranean Sea before and after the peak of the Messinian Salinity Crisis. *Palynology* 33 (2): 105–134. https://doi.org/10.1080/01916122.2009.9989688.

Raffi I, Backman J, Fornaciari E, Pälike H, Rio D, Lourens L *et al.* 2006. A review of calcareous nannofossil astrobiochronology

encompassing the past 25 million years. Quatern Sci Rev 25: 3113–3137. https://doi.org/10.1016/j.quascirev.2006.07.007.

Riding R, Braga JC, Martin JM, Sanchez-Almazo IM. 1998. Mediterranean Messinian salinity crisis: constraints from a coeval marginal basin, Sorbas, southern Spain. *Mar Geol* 146: 1–20. https://doi.org/10.1016/S0025-3227(97) 00136-9.

Rouchy JM. 1982a. La genèse des évaporites Messiniennes de Méditerranée. *Mém Muséum Nat Hist Nat*. Paris, Série C, Sciences de la Terre, L, 280 p.

Rouchy JM. 1982b. La crise évaporitique messinienne de Méditerranée : nouvelles propositions pour une interprétation génétique. *Bull Mus Nation Hist Nat* Paris, c, 3-4: 1–52.

Rouchy JM, Caruso A. 2006. The Messinian salinity crisis in the Mediterranean Basin: a reassessment of the data and an integrated scenario. *Sediment Geol* 188/189: 35–67. https://doi.org/10.1016/j.sedgeo.2006.02.005.

Rouchy JM, Caruso A, Pierre C, Blanc-Valleron MM, Bassetti MA. 2007. The end of the Messinian salinity crisis: Evidences from the Chelif Basin (Algeria). *Palaeogeogr Palaeoclimatol Palaeoecol* 254: 386–417. https://doi.org/10.1016/j.palaeo.2007.06.015.

Rouchy JM, Saint Martin JP. 1992. Late Miocene events in the Mediterranean as recorded by carbonate-evaporite relations. *Geology* 20 (7): 629–632.

Roveri M, Manzi V, Bergamasco A, Falcieri FM, Gennari R, Lugli S *et al.* 2014a. Dense shelf water cascading and Messinian canyons: a new scenario for the Mediterranean salinity crisis. *Am J Sci* 314: 751–784. https://doi.org/10.2475/05.2014.03.

Roveri M, Flecker R, Krijgsman W, Lofi J, Lugli S, Manzi V *et al.* 2014b. The Messinian salinity crisis: past and future of a great challenge for marine sciences. *Mar Geol* 352: 25–58. https://doi.org/10.1016/j.margeo.2014.02.002.

Roveri M, Gennari R, Lugli S, Manzi V, Minelli N, Reghizzi M *et al.* 2016. The Messinian salinity crisis : Open problems and possible implications for Mediterranean petroleum systems. *Pet Geosci* 22: 283–290. https://doi.org/10.1144/petgeo 2015-089.

Roveri M, Gennari R, Lugli S, Manzi V. 2009. The terminal carbonate complex: the record of sea-level changes during the Messinian salinity crisis. *GeoActa* 8: 67–77.

Roveri M, Lugli S, Manzi V, Reghizzi M, Rossi FP. 2020. Stratigraphic relationships between shallow-water carbonates and primary gypsum: insights from the Messinian succession of the Sorbas basin (Betic Cordillera, Southern Spain). Sedim Geol 404 (105678): 1–18. https://doi.org/10.1016/j.sedgeo.2020.105678.

Roveri M, Lugli S, Manzi V, Schreiber BC. 2008. The Messinian Sicilian stratigraphy revisited new insights for the Messinian salinity crisis. *Terra Nova* 20 (6): 483–488. https://doi.org/10.1111/j.13653121.2008.00842.x.

Rubino JL, Haddadi N, Camy-Peyret J, Clauzon G, Suc JP, Ferry S *et al.* 2010. Messinian Salinity Crisis expression along North African margin. *SPE Conference, Le Caire*, 129526 p.

Saint Martin JP, Cornée JJ, Conesa G, Bessedik M, Belkebir L, Mansour B *et al.* 1992. Un dispositif particulier de plate-forme carbonatée messinienne : la bordure méridionale du bassin du Bas Chélif (Algérie). *CR Acad Sci*, Paris, 315 (2): 1365–1372.

Saint Martin JP, Cornée JJ, Muller J. 1995. La disparition des récifs coralliens en Méditerranée à la fin du Messinien : un événement écologique majeur. In : La Méditerranée : variabilité climatique, environnement et biodiversité. Conference : *Okeanos*, Montpellier, xx pp. 70–74. https://www.researchgate.net/publication/262008605.

Saint Martin JP, Rouchy JM. 1990. Les plates-formes carbonatées messiniennes en Méditerranée occidentale : leur importance pour la reconstitution des variations du niveau marin au Miocène terminal. *Bull Soc Géol Fr* (8), VI, 1: 83–94.

Saint Martin JP. 1990. Les formations récifales coralliennes du Miocène supérieur d'Algérie et du Maroc. *Mém Mus Nat Hist Nat* Paris, 56: 366.

Satour L, Lauriat-Rage A, Belkebir L, Bessedik M. 2013. Biodiversity and taphonomy of bivalves assemblages of the Pliocene of Algeria (Bas Chelif basin). *Arab J Geosci*. https://doi.org/10.1007/s12517-013-1154-4, ISS N1866-7511.

Satour L, Saint Martin JP, Belkebir L, Bessedik M. 2020. Evolution de la diversité des bivalves messiniens de la bordure méridionale du bassin de Bas Chélif (Algérie nord occidentale). *Rev Paléobiol*, Genève, 39 (1): 249–263.

Satour L. 2021. Palaeoenvironmental distribution of late Miocene oysters in the northwestern Algerian basins. Arab J Geosci 14 (1890): 1–15. https://doi.org/10.1007/s12517-021-08248-z.

Sissingh W. 1972. Ostracodes from the sahelian near Carnot, N. Algeria. *Kkl Nederl Akad Wetensch* Amsterdam, *Proc Sér B*,75 (1): 84–95.

Sissingh W. 1976. Tentative middle Miocene to Holocene Ostracode biostratigraphy of the central and eastern Mediterranean basin, I, II. *Kkl Nederl Akad Wetensch*, Amsterdam, *Proc Sér B*, 79 (4): 271–299.

Snel E, Mărunţeanu M, Meulenkamp JL. 2006. Calcareous nannofossils biostratigraphy and magnetostratigraphy of the Upper Miocene and Lower Pliocene of the Northern Aegean (Orphanic Gulf-Strymon Basin areas), Greece. *Palaeogeogr Palaeoclimatol Palaeoecol* 238: 125–150. https://doi.org/10.1016/j.palaeo.2006.03.022.

Spadini V. 2019. Pliocene scleratinians from Estepona (Malaga, Spain). Atti Soc Tosc Sci Nat Mem, *Serie A*, 126: 75–94, https://doi.org/10.2424/ASTSN.M 2019.14.

Sprovieri R, Sprovieri M, Caruso A, Pelosi N, Bonomo S, Ferraro L. 2006. Astronomic forcing on the planktonic foraminifera assemblage in the Piacenzian Punta Piccola section (southern Italy). *Paleoceanography* 21, PA4204: 1–21. https://doi.org/10.1029/2006 PA001268.

Sprovieri R. 1993. Pliocene-early Pleistocene astronomically forced planktonic foraminifera abundance fluctuations and chronology of Mediterranean calcareous plankton bio-events. *Riv Ital Paleontol Stratigr*, 99, 3: 371–414. https://doi.org/10.13130/2039-4942/8903.

Stoica M, Krijgsman W, Fortuin A, Gliozzi E. 2016. Paratethyan ostracods in the Spanish Lago-Mare: More evidence for interbasinal exchange at high Mediterranean Sea level. *Palaeogeogr Palaeoclimatol Palaeoecol* 441: 854–870. https://doi.org/10.1016/j.palaeo.2015.10.034.

Suc JP, Do Couto D, Melinte-Dobrinescu MD, Macaleţ R, Quillévéré F, Clauzon G *et al.* 2011. The Messinian Salinity Crisis in the Dacic Basin (SW Romania) and early Zanclean Mediterranean-Eastern Paratethys high sea-level connection. *Palaeogeogr Palaeoclimatol Palaeoecol* 310, 3, 4: 256–272. https://doi.org/10.1016/j.palaeo.2011.07.018.

Suc JP, Popescu SM, Do Couto D, Clauzon G, Rubino JL, Melinte-Dobrinescu MC *et al.* 2015. Marine gateway vs. fluvial stream within the Balkans from 6 to 5 Ma. Mar Pet Geol 66: 231–245. https://doi.org/10.1016/j.marpetgeo.2015.01.003.

Tchouar L. 2013. Etude des dinoflagellés de la série mio-pliocène du Télégraphe de Sidi Brahim (Bassin du Chélif, Algérie nord occidentale) : systématique et Paléoécologie. *Magister thesis*, Oran 2 University, pp. 1–111.

Thomas G. 1985. Géodynamique d'un bassin intramontagneux. Le bassin du Bas Chélif occidental durant le mio-plio-quaternaire. *Thèse Doctorat d'Etat*, Université de Pau & Pays de l'Adour, 594 p.

Thunell RC. 1979. Climatic evolution of the Mediterranean Sea during the last 5.0 million years. *Sediment Geol* 23: 67–79.

Uliczny F. 1969. Hemicytheridae und Trachyleberididae (Ostxacoda) aus dem Pliozän der Insel Kephallinia (Westgriechenland). *Typo-Druck-Dienst édit*., Mtlnchen, 163 p.

Van Dijk G, Maars J, Andreetto F, Hernández-Molina FJ, Rodríguez-Tovar FJ, Krijgsman W. 2023. A terminal Messinian flooding of the Mediterranean evidenced by contouritic deposits on Sicily. Sedimentology, in press https://doi.org/10.1111/sed.13074.

Vertino A, Stolarski J, Bosellini FR, Taviani M. 2014. Mediterranean corals through time: from Miocene to present. In Goffredo S, Dubinsky Z. eds. The Mediterranean Sea: Its history and present challenges. Springer. 14: 257–274. https://doi. org/10. 1007/ 978-94-007-6704-1_14.

Vidal L, Bickert T, Wefer G, Röhl U. 2002. Late Miocene stable isotope stratigraphy of SE Atlantic ODP Site 1085: Relation to Messinian events. *Mar Geol* 180: 71–85.

Welter, Baures, Bougourd, Vidal, de Monvel, Seignier, Jouannuc. 1959. Carte géologique de Renault (n° 104) au 1/50 000è. Service géographique de l'Armée.

Zachariasse WJ. 1975. Planktonic foraminiferal biostratigraphy of the late Neogene of Crete (Greece). *Utrecht Micropaleont Bull* 11: 1–171.

Zibrowius H. 1980. Les Scléractiniaires de la Méditerranée et de l'Atlantique nord-oriental. *Mém Inst Océanogr* 11: 1–227.

Cite this article as: Atik A, Mansouri MEH, Bessedik M, Osman MK, Belkebir L, Saint Martin J-P, Chaix C, Belkhir A, Gorini C, Belhadji A, Satour L.. 2024. New insights on the latest Messinian-to-Piacenzian stratigraphic series from the Dahra Massif (Lower Chelif Basin, Algeria): Lago Mare, reflooding and bio-events, *BSGF - Earth Sciences Bulletin* 195: 2.